STRUCTURE, FACIES, AND INTERNAL PROPERTIES OF THE FRIO 'A' RESERVOIR, HITCHCOCK N. E. FIELD, GALVESTON COUNTY, TEXAS

Annual Report

By M. P. R. Light
assisted by W. D'Attilio

Prepared for the
Gas Research Institute
Contract No. 5084-212-0924

Bureau of Economic Geology
W. L. Fisher, Director
The University of Texas at Austin
Austin, Texas 78713

June 1985

DISCLAIMER

LEGAL NOTICE This report was prepared by the Bureau of Economic Geology as an account of work sponsored by the Gas Research Institute (GRI). Neither GRI, members of GRI, nor any person acting on behalf of either:

a. Makes any warranty or representation, express or implied, with respect to the accuracy, completeness, or usefulness of the information contained in this report, or that the use of any apparatus, method, or process disclosed in this report may not infringe privately owned rights; or

b. Assumes any liability with respect to the use of, or for damages resulting from the use of, any information, apparatus, method, or process disclosed in this report.

RESEARCH SUMMARY

Title	Structure, Facies, and Internal Properties of the Frio 'A' Reservoir, Hitchcock N.E. Field, Galveston County, Texas.
Contractor	Bureau of Economic Geology, The University of Texas at Austin, GRI Contract No. 5084-212-0924.
Principal Investigator	R. J. Finley/R. A. Morton
Report Period	May 1, 1984-July 31, 1985
Objective	To evaluate the mechanism of secondary gas recovery by co-production in a slightly geopressured watered-out reservoir. This involved making a geologic interpretation of the field and defining the reservoir parameters adequately for reservoir engineering and modeling analysis. To investigate the potential for shale dewatering occurring as a result of fast pressure drawdown during co-production of gas and water. To investigate the hydrocarbon sources for gas and condensate, i.e., whether they are locally derived or have migrated from deeper levels.
Technical Perspective	The Hitchcock N.E. field was placed in a regional context, especially the facies and structure of the Frio 'A' sandstone. Emphasis was placed on the facies influence on reservoir continuity, porosity, and permeability as well as the diagenetic modification of porosity and permeability. Shale dewatering was examined in the context of three types of fluid movement: original migration of hydrocarbons, shale dewatering from burial, and pressure drawdown due to production. The source of the gas and condensate is being investigated by a number of geochemical techniques.
Results	The N. E. Hitchcock field, which produces from the Frio 'A' or 9,100 ft sandstone, is defined by a northwest plunging anticline of moderate relief. It is truncated on its southeast flank by a major fault downthrown several hundred feet to the south. Several minor faults displace the original pay zone and may influence enhanced gas recovery efforts in the reservoir. The Frio 'A' sandstone, which occurs at the top of the Frio Formation in the Chocolate Bayou area, forms part of a constructive delta lobe in the N. E. Hitchcock field. It consists of a stacked sequence of distributary-mouth-bar sandstones which grades into a thin delta destructional unit and is overlain by the transgressive shallow-marine Anahuac shale. Marine reworking of the Frio 'A'

sandstone has resulted in its broad lateral extent and internal continuity although thin shale breaks vertically partition the reservoir. Much of the preserved excellent porosity (± 30%) and permeability (± 1,000 md, 0.99 μm^2) in the Frio 'A' sandstone is due to its distributary-mouth-bar origin. The porosity and permeability were subsequently modified by diagenetic reactions.

The Frio 'A' aquifer extends some eight miles southwest of the N. E. Hitchcock field to the Alta Loma and Sarah White fields. It is confined on its northern and southern flanks by major growth faults. The continuity of the Frio 'A' sandstone has bearing on any plans to control water influx by drilling additional guard wells below the gas-water contact. However, reservoir modeling suggests that the faults are not sealing during co-production pressure drawdown.

Variable areas of indurated authigenic kaolinite zones developed in the Frio 'A' sandstone adjacent to thin shale units probably result from fluids emitted from the shales which have a consistent illite-smectite composition. Slight reductions in salinity during production at the Prets No. 1 well may be evidence for contemporaneous dewatering of shales.

Shale pyrolysis data indicate that the Anahuac and Frio shales are of too poor a quality and are too immature to have generated appreciable hydrocarbons. Furthermore isotope data for the Prets No. 1 condensates imply a marine organic source for these fluids. Thermal and hydrocarbon maturity data indicate that the Upper Frio was subjected to an extended period of hot, extremely saline, basinal-fluid flow. This fluid flow appears to have introduced the hydrocarbons, and caused albitization of feldspars and formation of carbonate cements.

Technical Approach

Base maps and a selected number of well logs were acquired in order to prepare new cross sections and maps illustrating the stratigraphic characteristics of the Frio 'A' sandstone. Depositional systems and constituent facies were defined from maps and cross sections in conjunction with published information (Galloway and others, 1984). Detailed geologic mapping of the Frio 'A' sandstone, and a detailed description of a core cut in the Delee No. 1 well were conducted to estimate the size, extent and compartmentalization of the reservoir for simulation purposes. Shale Frio 'A' sandstone compositional changes were examined by a number of techniques at the Frio 'A' sandstone boundary for evidence supporting shale dewatering and the diagenetic history of Frio sandstones. Forty shale samples were subjected to total organic carbon and Rock-Eval pyrolysis analyses. These data give an indication of the quantity of hydrocarbons in the shales (and hence available during shale dewatering) and the shale thermal maturity. Detailed gas chromatography-mass spectrometry analyses are presently being done on samples of gas and condensate from the Prets and Delee No. 1 wells. These data should bear on the source of the hydrocarbons. The hydrogen and oxygen isotope ratios of formation waters coexisting with hydrocarbons in the Prets

No. 1 and Delee No. 1 wells are being measured and will be used to define the source of the waters.

Project Implications

CONTENTS

Figures

Tables

INTRODUCTION

Investigations into the feasibility of gas production from watered-out reservoirs have developed from research into the production of gas from hot brines in geopressured aquifers along the Gulf Coast (Dorfman, 1982). Dorfman (1982) predicted that watered-out gas reservoirs would become more important as an economic source of natural gas. Co-production of watered-out, hydropressured gas reservoirs and geopressured prospects appears to be economically viable (Gregory and others, 1983).

Co-production of oil with geopressured gas could significantly improve the economic prospects of gas utilization thus improving the reserves of both energy resources (Weres and others, 1984).

As part of GRI's Unconventional Natural Gas Research Program, the Bureau of Economic Geology and the Center for Energy Studies, both located at The University of Texas at Austin, have contributed to a joint project on the Hitchcock N.E. field (Galveston County). This project was entitled "Coordination of Geological and Engineering Research in Support of Gulf Coast Co-production" and involved the following research objectives.

1) Placing the Hitchcock N. E. field in a regional context, especially the facies and structure of the Frio 'A' reservoir sandstone. During 1984 the Frio 'A' (9,100 ft or top Frio) sandstone was correlated in more than 200 electric logs over the Hitchcock, Hitchcock N.E., Alta Loma, Sarah White, and Chocolate Bayou oil and gas fields. Regional sandstone distribution (thickness and percentage) maps and facies maps have been drawn which tie the Hitchcock N.E. field to the Chocolate Bayou field (Brazoria County) to the west. The Frio 'A' sandstone is represented by two units in many areas and these have been mapped separately and in combination. The sandstone distribution and facies maps allow an assessment to be made of the depositional environment of the Frio 'A' sandstone.

2) Detailed geologic mapping (structure, gross sandstone thickness, and net sandstone thickness above original gas-water contact) of the Frio 'A' sandstone in the Hitchcock N.E.

field was needed to understand the size, extent, and compartmentalization of the reservoir for simulation purposes. Local cross sections were constructed over the Hitchcock N.E. field in an attempt to determine the degree of reservoir compartmentalization. A search was made for thin shale breaks/permeability barriers which may be important during rapid drawdown relative to long-term primary production. The completed maps were made available to the Center for Energy Studies who then modeled the Hitchcock N.E. reservoir using the pressure drawdown enhancement technique.

3) An examination was made of the potential for shale dewatering occurring as a result of fast pressure drawdown during co-production of gas and water. This shale water would help to replenish pressure. This entails discriminating between three types of fluid movement:

a) Original migration of hydrocarbons from the source and emplacement in the trap.

b) Shale dewatering as a consequence of compaction and pressure/temperature increase due to burial effects.

c) Shale fluid flow (dewatering) during production.

In 1984 the Secondary Gas Recovery Delee No. 1 co-production well penetrated the Frio 'A' (9,100 ft) reservoir sandstone in the Hitchcock N.E. field. One hundred and thirty feet (40 m) of core were cut over this depleted gas-condensate accumulation, of which the upper 34.5 feet (10.5 m) consisted of the overlying Anahuac Formation shales. A detailed correlation between rate of penetration of the drill bit and the induction logs had been maintained prior to coring to accurately fix the core position. Cuttings samples were also collected over the whole interval from lower Miocene to total depth in this well. A detailed core description was made on site and the core examined under ultraviolet light for the presence of liquid hydrocarbons.

The availability of shale samples at some distance from, adjacent to, and within the Frio 'A' sandstone as a result of this coring operation allowed shale dewatering to be investigated by several approaches.

Shale compositional changes were examined at the Frio 'A' sandstone boundaries and adjacent thin shale layers within the reservoir using Scanning Electron Microscope (SEM) and Energy Dispersive Spectrometer (EDS) techniques, X-ray diffraction, inductively-coupled-plasma analysis (elemental), and detailed core descriptions at our laboratories. Shale compositions were estimated and a large number of cross plots and ternary diagrams constructed of elemental composition, elemental ratios, and other parameters. These data were then examined for any evidence supporting shale dewatering.

Compositional changes within the Frio 'A' sandstone were also investigated using the SEM-EDS technique as well as by doing a detailed core description. Thin shale or permeability barriers were recorded during this procedure. A search was made for zones showing excessive authigenic cementation which might be evidence of either shale dewatering or original fluid movement during migration of hydrocarbons into the reservoir. This information has been combined with diagenetic models for the Frio Formation and has been used to decipher the diagenetic history of the Frio 'A' sandstone. The clay composition, sequence, and distribution bear on permeability variation and quality in the reservoir.

Detailed petrographic work is still to be done on the samples analyzed with the SEM-EDS. Four samples of sandstone were also subjected to inductively-coupled-plasma elemental analysis to estimate the concentrations of certain elements with large neutron-capture cross sections. These data were made available to Dr. H. Dunlap for calibration of certain logs in the Delee No. 1 well.

4) An investigation was conducted on the source of the gas and condensate in the Frio Formation with particular emphasis on the Hitchcock N.E. field. This is a continuation of an integrated geologic study of the Pleasant Bayou-Chocolate Bayou area,

Brazoria County, Texas, sponsored by the U.S. Department of Energy. The purpose of this research was to determine whether the hydrocarbons present in the Hitchcock field are locally derived by shale dewatering or have migrated up from deeper levels. Should the hydrocarbons have a local derivation, there could be an additional influx from the shales by fast pressure drawdown during production. The methods followed in this investigation are outlined below.

The thermal maturation of the Anahuac shales, shale stringers within the Frio 'A' sandstones, and Frio shales below the Frio 'A' sandstone was studied. Vitrinite reflectance analyses were conducted on forty shale samples from this interval by Robertson Research (U.S.) Inc., and their data are given in the appendix. The vitrinite reflectance data were combined with modeled thermal maturity using the present geothermal gradient in the Hitchcock N.E. field area and hydrocarbon maturity using the naphthene concentration in the oils to estimate the depth at which the hydrocarbons formed. Shale samples near the Frio 'A' sandstone were examined for the thermal effects of migrating hot-hydrocarbon bearing fluids.

Forty shale samples were subjected to total organic carbon and Rock-Eval pyrolysis analyses by Geochem Laboratories, Inc., and these analyses are listed in the appendix. These data have given an indication of the quantity of hydrocarbons present in the shales (and hence available during shale dewatering), the amount released by pyrolysis, the relative amount of oxygen and hydrogen in the kerogen, and its thermal maturity. An indication of the kerogen quality and its hydrocarbon productivity bears on the local derivation of hydrocarbons in the Hitchcock N.E. field.

Detailed gas-chromatography-mass spectrometry analyses are presently being done by Geochem Laboratories, Inc., on samples of gas and condensate from the Phillips Prets No. 1 and S.G.R. Delee No. 1 wells, Hitchcock N.E. field. It was hoped that these data would be available at the time of writing this report. However, considerable delay in

starting production on the Delee No. 1 well has resulted in only preliminary analyses being available. The entire analysis procedure is outlined in the appendix.

The C_4-C_7 gasoline range and C_{15}+ paraffin-naphthene (P-N) gas-chromatography analyses and C_{15}+ gas chromatography-mass spectrometry analyses will be correlated with Geochem source rock extract analyses at the Pleasant Bayou No. 1 well (Brazoria County) over the entire sampled interval (2,072 ft-16,500 ft, 630 m-5,030 m). These analyses should indicate whether or not the hydrocarbons are derived from Oligocene sediments.

The C_4-C_6 gasoline range data have been and will be used to estimate the maturity of the sediments using the methods of Young and others (1977). Biomarker analyses will be used to investigate the geological environment of the source rocks and hence assist in fixing its probable location when combined with depth data from other work.

Detailed carbon and hydrogen isotope analyses of the gases and condensates from the Prets No. 1 and Delee No. 1 wells are being conducted by Coastal Science Laboratories, Inc. (Table 1). These data will give an estimate of the temperature of formation (maturity of the source rock) and the depositional environment of the source rocks. It may be possible to estimate the effects of migration and mixing using the methods of Schoell (1983). Geothermal gradient and vitrinite reflectance data from the Hitchcock N.E. field have been combined with hydrocarbon maturity in estimating a depth of hydrocarbon generation.

The hydrogen and oxygen isotope ratios of the formation waters co-existing with the hydrocarbons in the Prets No. 1 and Delee No. 1 wells are being measured and will be compared to isotopic ratios from authigenic cements in Brazoria County and other oil fields in the Gulf Coast (Loucks, Richmann, and Milliken, 1981). Some data already exist and are discussed in this report. Isotopic data are used to define the source of the waters (Table 1).

Table 1. Isotope Analyses of Hydrocarbons and Formation Waters, Hitchcock N. E. Field.

$\delta^{13}C$ and $\delta^{2}H$, methane:

$\delta^{13}C$, gas components (C_2, C_3, C_4, C_5, CO_2):

δ^{13}/C, condensate:

$\delta^{18}O$ and $\delta^{2}H$, water:

Isotopes	Large Component from Shale Dewatering	Large Component from Basinal Brines
Oxygen $\delta^{18}O$	Heavy $\delta^{18}O$ for quartz overgrowing indicates formation at shallower depths	$\delta^{18}O$ constant in formation fluid with depth - no indication of source of formation fluid
Hydrogen δD	Constant?	δD becomes depleted with increasing depth of formation fluid
Carbon $\delta^{13}C$	Constant?	$\delta^{13}C$ becomes depleted over temperature range 100° to 120°C (212° to 215°F) and then increases with increasing depth
$\delta^{18}O$ V's δD		Distinguishing genetic groups of waters
$\delta^{18}O$ V's $\delta^{13}C$		Distinguishing genetic groups of waters
Sulfur $\delta^{34}S$		Formation water source identification

The nickel and vanadium contents of the oils at the Prets No. 1 and Delee No. 1 wells are being measured by Geochem Laboratories, Inc., and will be of use when additional work is done on oil-source rock correlations in the Frio and older formations.

This report presents the results of investigations into the structural, stratigraphic, facies and diagenetic controls of porosity and permeability in the Hitchcock N.E. field. These data bear on the size and continuity of the field and the best location for guard wells to reduce water influx into this depleted reservoir, and the degree of shale dewatering occurring during pressure drawdown.

Regional Setting

The Hitchcock N.E. field lies beneath part of the townsites of Hitchcock and LaMarque in Galveston County some 15 miles (9 km) northwest of the City of Galveston (fig. 1). The producing reservoir (Frio 'A', or 9,100 ft) sandstone is widely distributed in a belt parallel to the Texas coastline and has produced from many fields along the Texas Gulf Coast and southern Louisiana (Anderson and others, 1984).

The Frio 'A' sandstone occurs below the T2 marker horizon at the top of the Oligocene Frio Formation. The geostatic gradient is about 0.6 psi/ft (13.6 kPa/m) at the level of the Frio 'A' reservoir (fig. 2) which has an average temperature of 215°F (101°C) (fig. 3). However, the top of the geopressured zone occurs about 7,200 ft (2,200 m) below sea level at the Hitchcock N.E. field, some 400 ft (120 m) below the top of the Anahuac Formation (fig. 2). This reservoir is slightly geopressured in contrast to the Mt. Selman co-production test which was normally pressured.

The Hitchcock N.E. field is located on the seaward fringe of the Houston Delta system (fig. 4). The following discussion of the regional geology is from Galloway and others (1982). Several minor, laterally coalesced, vertically repetitive deltaic cycles compose the Houston Delta system which is the main locus of terrigenous accumulation in the Frio. Elongate to lobate deltas formed during the most regressive phases in the Lower

Frio and more arcuate deltas during periods of general transgression and shoreline retreat in the upper Frio (Galloway and others, 1982).

During middle Frio deposition, deltas were supplied by large fluvial channel systems (Chita-Corrigan Fluvial System) some 16 to 20 miles (25 to 33 km) north and west of the Hitchcock N.E. field. Net-sand isopachs show that the positions of the fluvial axes changed substantially with time (Galloway and others, 1982).

Platform-delta sequences from 50 to 300 ft thick (15 to 90 m) characterize the middle and upper Frio in the Houston Delta system. Blocky sandstones record the development of multistoried wave-reworked sandstones of recurrent delta-destructional phases. The deltas became smaller as successive lobes shifted landward. Transgression and wave-reworking produced thick time-transgressive blanket sandstones. There was constant switching of the delta lobes, destructional marine reworking, and inundation of the abandoned sites (Galloway and others, 1982).

The depositional style of the Upper Frio was strongly influenced by the Anahuac marine transgression. This shale wedge, which pinches out updip, marks the invasion of a comparatively sediment-starved shelf and contains a neritic fauna. In part it was deposited contemporaneously with and is indistinguishable from the Upper Frio prodelta muds (Galloway and others, 1982).

Structure

During Frio deposition growth faulting produced a closely spaced pattern of strike-parallel, broadly arcuate fractures (Galloway and others, 1982). The Frio 'A' aquifer at the N. E. Hitchcock field occurs within an ovoid fault block some 10.5 miles (17 km) long and 4.6 miles (7 km) wide (fig. 5). Isolated circular to ovoid areas of thick sand accumulation may represent sites of major growth faulting or salt-withdrawal basins (Galloway and others, 1982). The fault block lies within an area characterized by deeply buried salt diapirs (T. E. Ewing, personal communication, 1985).

The Hitchcock N.E. field is defined by a northwest plunging anticline of moderate relief (fig. 6). It is truncated on its southeast flank by a major northeast trending growth fault with several hundred feet of throw. This fault forms the southern boundary of the reservoir and aquifer (figs. 5 and 6).

A fault wedge upthrown some 50 ft forms the northwest flank of the field. This wedge formed contemporaneously with Frio 'A' sandstone deposition as there is a marked change in sandstone thickness and facies across it. Three other arcuate, northeast trending normal faults dissect the east flank of the reservoir and have throws which vary from 30 to 60 ft (9 to 18 m) (fig. 6). The two western faults appear to have isolated the Cockrell No. 1-Lowell Lemm well from both the Phillips No. 1 Prets well to the west and other wells to the east (Anderson and others, 1984; W. A. Parisi, personal communication, 1984, fig. 6).

A major east-west scissor fault (concave to the north) lies directly south of the Secondary Gas Recovery (S.G.R.) No. 1 Delee well (fig. 6). Though its throw exceeds 100 ft (30 m) in the west, its displacement decreases to 30 ft (9 m) over the crest of the structure (fig. 6). Two other en echelon scissor faults dissect the original Frio 'A' pay zone in the southern part of the Hitchcock N.E. anticline (fig. 6). However, the throw on these faults is less than 50 ft (15 m) on the western flank of the reservoir (fig. 6). These scissor faults do not disrupt the continuity of the reservoir which is evident from the subsurface pressure history. The whole region experienced an almost even pressure drop from the Phillips No. 1 Delaney (DE) in the north to the Phillips No. 1 Sundstrom (S) in the south over a 24 year period from 1957 to 1981 (Anderson and others, 1984).

Cores from the S.G.R. No. 1 Delee well indicate that thin shale and other permeability breaks appear to stratify the Frio 'A' reservoir (fig. 7). Larger shale breaks are also evident on electric logs from the Phillips No. 1 Prets and Thompson wells. Some of these breaks are clearly permeability barriers as they formed basal seals onto which heavier hydrocarbons have accumulated from gravity settling. This local vertical partitioning and the minor faults that isolate parts of the Frio 'A' reservoir possibly explain the different

oil-gas dew points and oil percentages found in PVT analyses of fluids from the Prets and Thompson wells. The location and throw of these minor faults and the position of shale breaks will influence enhanced gas recovery. Detailed mapping of the fault plane and juxtaposition of thin sandstone units should assist in identifying isolated sections of the reservoir and the best location for guard wells to reduce water influx into the reservoir.

Stratigraphy

Depositional Environment of the Frio 'A' Sandstone

In the Hitchcock N.E. field, the Frio 'A' sandstone consists of a stacked sequence of distributary-mouth-bar sandstones and thin delta destructional units and is overlain by the transgressive Anahuac shale (fig. 7). The facies distribution of the Frio 'A' sandstone has been analyzed using spontaneous potential (SP) profiles in an area extending from the Hitchcock N.E. field in the east to the Pleasant Bayou field some 11.5 miles (18.4 km) to the west. All major sandstone systems in the Hitchcock N.E. area exhibit a transition from thick, composite upward-coarsening sandstones updip to serrate sandstones downdip (fig. 8). The well-defined lobate to elongate net-sandstone thickness pattern (fig. 9) is evidence for deposition in a high-constructive lobate delta.

A distributary appears to have prograded some 3 miles (5 km) southeastward from the fault wedge forming the northwest flank of the Hitchcock N.E. field during the deposition of the Frio 'A' sandstone. This distributary progressively formed a major distributary-mouth-bar deposit on the southern downthrown block of the fault wedge. Further progradation resulted in deposition of a thickened sandstone on the downthrown southeast side of the major growth fault forming the southern boundary of the Hitchcock N.E. reservoir (figs. 8 and 9). SP profiles of distributary-mouth-bars are thinner and generally upward fining within the northwest fault wedge indicating their proximity to the distributary system. Thicker, composite upward-coarsening SP profiles are present in the south

and east of the Hitchcock N.E. field. Continuous delta front sandstones occur in more distal positions (fig. 8).

Facies Influence on Reservoir Continuity

Normally distributary-mouth-bar sandstones are composed of cross-stratified sandstones and silts displaying a wide variety of primary sedimentary structures (Coleman and Prior, 1980). The general lack of such structures and the massive nature of the Frio 'A' sandstone in the Hitchcock N.E. field is considered evidence for vigorous marine reworking. The strong marine influence resulted in the broad lateral extent and good internal continuity of the 'A' sandstone. The continuity of the Frio 'A' sandstone over the whole region must be considered in the placement of guard wells to control water influx.

The northeast orientation of the major growth faults strongly influenced sandstone thickness trends in the Frio 'A' aquifer as well as routes of water movement from the southwest. Hence guard wells should be located between fracture systems on the southwest side of the reservoir to effectively reduce the influx of water. Any attempts to isolate the Hitchcock N.E. field from the aquifer by fracturing and grouting must take account of the preferential orientation of fracture systems in the region. Should fracture systems accidentally be formed in the field, the flow characteristics of the reservoir may be severely affected by grouting.

Facies Influence on Porosity and Permeability

Modern and ancient distributary mouth-bars are commonly composed of medium to fine-grained well-sorted sand with large primary sedimentary structures and thus compose favorable potential reservoirs for hydrocarbons (Morton and others, 1983; Coleman and Prior, 1980). Much of the preserved excellent porosity ($\pm$ 30%) and permeability ($\pm$ 1,000 md, 0.99 μm^2) in the Frio 'A' sandstone is due to its distributary-mouth-bar origin (Table 2).

The permeability and porosity pattern for the Frio 'A' sandstone in the S.G.R. No. 1 Delee core shows a general upward decrease which is normally characteristic of an upward fining pattern (pattern 2, Morton and others, 1983, Table 1). However, grain size measurements of the mouth-bar sandstones in the cored interval indicate a consistent medium grain size (fig. 7). This implies either an upward decrease in sorting or an increase in diagenetic cements.

Within the massive distributary mouth-bar sandstones the upward decrease in permeability appears to be controlled by an increase in the calcite cement content, though occasional very thin carbonaceous layers are present. The lower mouth-bar sandstones which contain only minor calcareous streaks display permeabilities up to 1,000 md (0.99 μm^2) whereas in the shallower well-cemented mouth-bar sandstone permeability is only a few hundred millidarcys.

Porosity and permeability are indirectly related to internal stratification because sediment structures are partly controlled by grain size (Morton and others, 1983; Pryor, 1973). In Oligocene sandstones the relative ranking of permeabilities from highest to lowest corresponds to (1) foresets and large-scale troughs, (2) horizontal and low-angle, parallel-inclined stratification, and (3) small-scale troughs and ripple stratification (Morton and others, 1983). This relationship is demonstrated by the difference in permeability between the upper calcite-cemented distributary-mouth-bar sandstones and the overlying transgressive sandstones. Permeabilities in the massive to indistinctly laminated mouth-bar sandstones are an order of magnitude greater than permeabilities in the transgressive sandstones. The latter sandstones are well stratified, more poorly sorted and commonly coarser grained (fig. 7).

Diagenetic Modification of Porosity and Permeability

Primary porosity and permeability at the Hitchcock N.E. field were subsequently modified by diagenetic reactions and leaching by organic acids. Based on regional investigations of diagenesis the following parageneses are indicated (Loucks and others,

1981). Early clay coats formed around quartz grains and feldspars were leached. This was followed by euhedral quartz overgrowth development and secondary leaching of pore spaces (fig. 10). Remaining feldspars were then albitized and kaolinite crystallized in leached pore spaces (Loucks and others, 1981) (fig. 10). At the Hitchcock N.E. field, iron-chlorite formation appears to postdate quartz overgrowths and framboidal pyrite on which it has formed. Radiating calcium sulfate crystals have formed on quartz overgrowths and appear to be related to crystallization of fluids during the drying out of the core. Gypsum is unstable at the Frio 'A' reservoir temperatures and pressures (Blatt and others, 1972).

Oil is present throughout the S. G. R. No. 1 Delee core from both above and below the original gas/water contact at $\pm$ 9,105 ft (2,775 m) BMSL (figs. 3 and 4). P. Randolph (personal communication, 1984) suggests that this oil possibly is being expelled from geopressured shale below the Frio 'A' sandstone.

Shale Dewatering

The potential for shale dewatering occurring as a result of pressure drawdown during production has been examined. This entails discriminating between three types of fluid movement.

a) Original migration of hydrocarbons from source and emplacement in a trap.

b) Shale dewatering as a consequence of compaction and pressure/temperature increase during burial.

c) Shale fluid flow (dewatering) during production.

Original Fluid Migration

Maturation data in shales can be used as an indicator of hot fluid flow in adjacent sandstones (Light, 1985; Tyler and others, 1985).

The Pleasant Bayou geopressured-geothermal test wells in Brazoria County display a maturity anomaly which cannot arise as a consequence of simple conduction (Ewing and others, 1984). The corrected maturity in the Upper Frio (above T5) appears much higher

than that indicated when the present (and apparent regional) geothermal gradient is applied to the burial history of those strata (fig. 11) (Ewing and others, 1984). In contrast the maturity of the Lower Frio (below T5) is consistent with the present geothermal gradient (fig. 11). The higher thermal maturity of the Frio (T2 to T5 succession) is believed a consequence of heating by updip migration of hot basinal fluids formed during compaction and diagenesis of slope shales (fig. 12) (Ewing and others, 1984; Burst, 1969). A reduction to almost normal pressure in the Upper Frio may have allowed fluid migration to occur, while fluid movement would have been slower or static in the highly geopressured Lower Frio (pre-T5 succession) (fig. 12). Consequently, the maturity of the Lower Frio was not increased (Tyler and others, 1985).

Maturity data from the Delee No. 1 well (Hitchcock N.E. field) suggest however that in general the Anahuac shales tend to be more mature above the Frio 'A' sandstone than Frio shales within the reservoir. This is evident when the thermal maturity estimated by vitrinite reflectance is compared to the theoretical thermal maturity using Lopatin's method (Waples, 1980) and a burial history model (figs. 13 and 14). An anomaly of this kind may be related to higher geopressure and consequent increased geothermal gradient in the Anahuac (fig. 15) (Lewis and Rose, 1970), but it clearly is not a result of increased geothermal gradient as a result of hot fluid flow in the Frio 'A' sandstone. The thermal anomaly above the Frio 'A' sandstone occurs some 1,000 ft shallower in the Delee No. 1 well than the anomaly in the Pleasant Bayou test wells (Ewing and others, 1983) and hot upwelling fluids may have cooled to ambient temperatures by the time they had reached these shallower levels. Evidence for a deep source for the Delee No. 1 fluids will therefore have to be sought in hydrocarbon compositional and isotopic data.

The composition of the hydrocarbons in oil change as they mature and this variation may be used to estimate the time of oil formation (Young and others, 1977). The calculation of hydrocarbon ages for the gasoline range hydrocarbons is based on the

apparent disproportionation of naphthenes to give paraffins and aromatics (Table 3) (Light, Tyler and Ewing, in prep.).

Young and others (1977) used 10 naphthenes (cyclopentane to ethylcyclopentane), 17 paraffins (isopentane to n. heptane), and 2 aromatics (benzene and toluene) in their calculations. They were unable to improve the accuracy of the method by deleting certain of the individual compounds or groups of compounds. Detailed C_4-C_7 hydrocarbon extract analyses from cuttings samples from the Pleasant Bayou test wells (Brazoria County) and gas/condensate/oil from the Prets No. 1 well Hitchcock N.E. field are available. These analyses include however only 9 naphthenes, 16 paraffins, and 2 aromatics (Brown, 1980). Though the calculated ages (fig. 16) for the Delee No. 1 and Pleasant Bayou test wells are not directly compatible with Young and others' (1977) data, the error is probably not large as almost the complete suite of gasoline range hydrocarbons is considered. The calculated age for the Prets No. 1 gasoline range hydrocarbons is older than the age of the formation in which they occur.

The basis of the hydrocarbon age calculation method assumes that the disproportionation reaction of naphthenes depends on the effects of time and temperature. The naphthene concentration (C_n) is related to time and temperature by the following equation (equation 5, table 3).

Natural logarithm C_n = intercept + slope x (time-temperature integral (TTI)) (Young and others, 1977).

This has been calibrated for gasoline-range hydrocarbons in clastic reservoirs (Young and others, 1977).

When the naphthene fractions of the Pleasant Bayou No. 1 well and Prets No. 1 well are expressed as TTI and are plotted against depth the highly geopressured lower Frio (pre T5 marker horizon) and some of the shallow Miocene have high naphthene concentrations (i.e., low maturity or TTI). Conversely, most of the Miocene, Anahuac, and Upper Frio show low naphthene concentrations (i.e., high maturity or TTI). The high maturities

Table 3. Disproportionation reaction for naphthenes.
From Reznikov, 1967.

Disproportionation reaction for naphthenes

$$4N = 3P + 1A \qquad (1)$$ (Reznikov, 1967)

Normalized naphthene concentration

$$Cn = \frac{N}{N+P+A} \qquad (2)$$

Time rate change of concentration

$$\frac{dC}{dt} = -KC \qquad (3)$$

Reaction rate "constant"

$$K = be^{-\frac{E}{RT}} \qquad (4)$$

Natural logarithm of normalized naphthene concentration

$$LnCn = -b \int_{t=0}^{t=t} e^{-\frac{E}{RT}} dt + a \qquad (5)$$

Time temperature index

$$TTI = \int_{t=0}^{t=t} e^{-\frac{E}{RT}} dt \qquad (6)$$

(equations 2-6 from Young and others, 1977)

N = naphthenes

P = paraffins

A = aromatics

R = universal gas constant

T = absolute temperature °K

b = constant

Cn = normalized naphthene concentration
t = time at which reaction concentration is C
K = reaction rate constant at temperature t
e = base of natural logarithmic system
E = activation energy of the reaction
a = constant (equal to LnC at t=0)

(TTI) shown by the hydrocarbons above the T5 marker horizon (Miocene, upper and middle Frio) compared to the thermal maturity of their containing sediments derived from the burial history indicate that these fluids have migrated up from more deeply buried, more mature source rocks (fig. 11). High geopressure below the T5 marker horizon probably arrested fluid flow and the hydrocarbons present are more locally derived. The discrepancy between the hydrocarbon maturity data and the burial history maturity profile below T5 in the lower Frio Formation may represent a standard error in the calculation of the maturity (TTI) from naphthene concentration.

The presence of an anomalous concentration of C_5-C_7 gasoline range hydrocarbons in the T3 to T5 succession in a zone of relatively low wetness is consistent with the idea that they have been introduced (Brown, 1980). The thermal maturity (vitrinite reflectance) above the top of the Frio is lower than the maturity of the hydrocarbons in their containing rocks (fig. 11). This is probably a consequence of the fluids having lost their heat to the surrounding formations by the time they had reached these shallower levels (fig. 11).

Shale Dewatering from Burial Effects

Shales tend to be water wet due to the preferential adsorption of water on grain surfaces because of strong electrostatic forces active between the fine clay grains and pore fluids (Hinch, 1980). The effect of adsorption is to cause "dynamic" structuring of the water close to the mineral grain surfaces (Hinch, 1980). The structured water close to the grain surfaces though highly mobile on a molecular scale is immobile in a hydrodynamic sense.

Shale water is lost by compaction due to burial until about only 10 layers of water molecules separates the clay grains near the top of geopressured shale (Hinch, 1980). After this movement of the hydrated ions is inhibited because they are close in size to the average pore size and the shales maintain a constant porosity (Hinch, 1980). However, Newton (in Hinch, 1980) noted that hydrocarbon accumulations in the Gulf Coast are

associated with waters having slightly subnormal salinity. This may be a result of dewatering of the surrounding geopressured shales (Hinch, 1980). The sandstones at the Frio 'A' level in the Delee No. 1 well are geopressured (geopressure gradient 0.6 psi/ft) while geopressure starts at 7,200 ft (2,200 m) some 1900 ft (580 m) shallower than the producing reservoir (fig. 2). We can therefore expect the shales surrounding the Frio 'A' sandstone at the Delee No. 1 well to have already entered a zone of fairly constant porosity and for the shale water to average around 2 to 10 layers separating clay grains (Hinch, 1980). Hinch (1980) has argued that the generation of hydrocarbons in the geopressured zone can result in an increase in water content. However, the very low total organic carbon content of the shales in the Delee No. 1 well (averaging 0.35% TOC) and immature nature of the woody hydrocarbons make water production difficult (see section on shale pyrolysis data).

The content of structural water within the shale can be estimated by the analysis of the hydrogen and carbon content of the products of shale pyrolysis at very high temperatures. These analyses will be done at the Mineral Studies Laboratory at the Bureau of Economic Geology in the next control period. The carbon and hydrogen content of shale organic material pyrolized at different temperatures should give a straight line which will intercept the hydrogen axis at 0% carbon. This intercept will give the remaining amount of hydrogen tied up in structured water. This structured water can be compared to the bound water estimated by log analysis and may be used to estimate the maximum amount of water available for shale dewatering.

Smectite begins to alter to illite when temperatures have exceeded 90 to 100°C (194°-212°F) and when potassium and aluminum are present in the pore waters (Foscolos and others, 1976; Powell and others, 1978). The temperature at the level of the Frio 'A' sandstone is close to this value (215°F, 101°C) in the Hitchcock N.E. field (fig. 3) (Light, 1985).

Early work had suggested that during the transformation of smectite to illite a mixed layer silicate formed in which aluminum substituted for silicon in the tetrahedral position promoting a charge deficit which resulted in potassium being absorbed on the clay surface. This potassium was believed to displace calcium, magnesium, or iron while water sloughed off into the solution (Foscolos and others, 1976; Powell and others, 1978). These changes were believed to be recognized by a reduction of the d001 spacing of a Ca-saturated smectite from 1.56 to 1.20 μm in the mixed layer clay (Foscolos and Powell, 1980).

The amount of water lost by dehydration during the smectite-illite transition was estimated at 270 to 290 mg per gram of clay (Mooney and others, 1952) which represents 10-15 percent of the compacted bulk volume of argillaceous sediments (Burst, 1969). This period of apparent clay dehydration coincides with a maturity level of 0.5% Ro (Foscolos and others, 1976; Powell and others, 1978). The maturity at the Delee No. 1 well at the level of the Frio 'A' sandstone exceeds this amount (± 0.6% Ro, fig. 14).

The Anahuac shales overlying the sandstones in the Delee No. 1 well were initially subjected to X-ray diffraction analyses in an attempt to find evidence to support clay dewatering during production. Nadeau and others (1984) have however demonstrated that materials representing commonly interstratified clay minerals are composed of aggregates of fundamental particles whose X-ray diffraction patterns result from interparticle diffraction. What was taken formerly to be randomly interstratified smectite-illite is composed of primary populations of illite and smectite particles (Nadeau and others, 1984). During diagenesis smectite particles become unstable and dissolve while illite particles are formed (Nadeau and others, 1984). When the smectite has completely gone, the remaining population consists of elementary illite and thicker illite particles which when examined under XRD appear to be regularly interstratified smectite-illite with 50% or more illite (Nadeau and others, 1984). Consequently the reduction in the (XRD) d001 spacing during the smectite-illite transformation can no longer be taken as an indication of the amount of

water lost by dehydration but is rather a measure of the change in elementary illite particle size.

ICP elemental analyses were conducted on seven shale samples from above, within, and at the base of the Frio 'A' sandstone by the Mineral Studies Laboratory at the Bureau of Economic Geology (Table 4). These data have been used in place of the XRD information to estimate the illite content of the shales. A ternary diagram showing the relative percentages of K_2O to CaO and Na_2O and Fe_2O_3 and MgO in the shales was constructed. These shale compositions were then compared to those of pure clay end-members from which the approximate illite percentage and the silica concentration in the shales was estimated (fig. 17) (Deer, Howie and Zussman, 1969). The illite percentage appears to be fairly erratic in the clays and lies mainly between 50 and 70%, while the silica content of the shales is more consistent (fig. 17).

The transformation of smectite to illite is potentially important if water and ions released by this reaction migrate into sandstones where they may affect diagenesis (Loucks, Richmann and Milliken, 1981).

Boles and Franks (1979) have showed that smectite-illite transformation reactions with aluminum as an immobile component release significantly more cations (silica release increases more than five times) than do reactions in which aluminum is considered a mobile component (Loucks, Richmann and Milliken, 1981). Provisional data had suggested that the aluminum had been mobile in the shales directly overlying the Frio 'A' sandstone (fig. 18) in the Delee No. 1 well. However additional SEM-EDS analyses of the clay fraction over this interval indicate that it has a very consistent illite-smectite composition. The apparent decrease in alumina appears entirely due to an increase in the content of detrital components in the clay (mostly quartz), a consequence of the upward-fining nature of the upper boundary of the Frio 'A' sandstone. Aluminum can therefore be considered immobile in the smectite-illite transformation reaction and this reaction in the Anahuac shales

Table 4. Inductively coupled plasma (ICP) analyses for shale samples from the S.G.R. Delee No. 1 well.

SAMPLE NO.		2	1	10	9
LAB. NO.		84-822	84-824	84-854	84-855
LOC ID		9092' SHALE	9070' SHALE	9194' 3" SHALE	9179' 11" SHALE
SiO_2	(Wt %)	63.95	62.76	66.76	61.27
Na_2O	"	1.71	1.66	2.04	1.73
K_2O	"	2.60	2.71	3.15	3.33
MgO	"	2.14	2.11	1.78	2.08
CaO	"	1.31	1.58	1.58	3.39
Al_2O_3	"	18.59	17.87	16.49	16.33
$Fe_2O_3(T)$	"	5.33	5.74	4.00	4.13
TiO_2	"	0.84	0.83	0.77	0.82
MnO	"	0.03	0.05	0.01	0.02
P_2O_5	"	<0.25	<0.25	<0.25	<0.25
TOTAL		96.50	95.31	96.58	93.10
Sr	"	250	280	160	270
Ba	"	460	360	290	430
Zr	"	180	180	510	210

LOC ID depth footage from Delee No. 1 well, Hitchcock N.E. field.

Table 4. (continued)

SAMPLE NO. / LAB. NO. / LOC ID		8 84-817 9100' 10.75" SHALE	6 84-819 9100' 6" SHALE	7 84-819(FINE) 9100' 6" SHALE	5 84-821 9099' 5.5" SHALE
SiO_2	(Wt %)	76.76	70.24	61.69	67.75
Na_2O	"	1.56	1.24	0.56	2.05
K_2O	"	1.91	2.15	2.60	2.68
MgO	"	1.30	1.30	2.63	1.82
CaO	"	1.50	0.83	0.70	1.67
Al_2O_3	"	10.95	12.97	19.92	16.50
Fe_2O_3	"	4.49	3.49	6.10	3.83
TiO_2	"	0.36	0.55	0.86	0.73
MnO	"	0.02	0.01	0.01	0.01
P_2O_5	"	<0.25	<0.25	<0.25	<0.25
TOTAL		98.85	92.78	95.07	97.04
Sr	"	260	250	150	300
Ba	"	450	1,020	740	410
Zr	"	*80	150	160	200

LOC ID depth footage from Delee No. 1 Well, Hitchcock N.E. field.

Table 4. (continued)

SAMPLE NO. LAB. NO.		DUPLICATES 3 84-822 9092' SHALE Run 1	DUPLICATES 4 Run 2	Cody Shale USGS SCO-1 Found	QUALITY ASSURANCE Accepted	Green River Shale-USGS SGR-1 Found	QUALITY ASSURANCE Accepted
SiO_2	(Wt %)	64.36	63.53	62.81	62.3?	28.73	28.3?
Na_2O	"	1.71	1.71	0.90	0.9?	3.00	3.0?
K_2O	"	2.60	2.59	2.74	2.7?	1.50	1.6?
MgO	"	2.14	2.14	2.63	2.6?	4.25	4.5
CaO	"	1.31	1.31	2.65	2.6?	8.57	7.2?
Al_2O_3	"	18.62	18.55	13.63	13.6?	6.53	6.5?
Fe_2O_3(T)	"	5.34	5.32	5.32	5.1?	3.05	3.2?
TiO_2	"	0.84	0.83	0.62	0.64?	0.26	0.26?
MnO	"	0.03	0.03	0.05	0.05?	0.03	0.03?
P_2O_5	"	<0.25	<0.25	* 0.21	0.29?	<0.25	0.4?
Sr	"	255	257	216	200?	502	500?
Ba	"	457	465	570	500?	260	300?
Zr	"	199	171	100	150?	<41	70?

LOC ID depth footage from Delee No. 1 Well, Hitchcock N.E. field.

directly above the Frio 'A' sandstones would release significant amounts of silica and other elements to the reservoir. The transformation reaction is outlined below.

$$\text{Smectite} + Al^{+3} + K^{+} = \text{illite} + \text{amorphous } Si^{+4} + \text{various amounts of } Ca^{2+}, Mg^{2+}, Fe^{2+} \text{ and interlayer } H_2O$$

(Hower and others, 1976)

The clay water containing amorphous silica probably migrated into the Frio 'A' sandstones during dewatering where the silica crystallized out as authigenic quartz overgrowths (Morton, 1983). These authigenic quartz overgrowths formed at temperatures of 75° to 80°C (167° to 176°F) in Brazoria County (Loucks, Richmann and Milliken, 1981).

Kaolinized feldspars and authigenic kaolinite cement are present throughout most of the Frio 'A' reservoir in the Delee No. 1 well. There does not seem to be a marked increase in kaolinite content in the upper parts of the reservoir as would be expected if major introduction of alumina rich fluids had occurred as a result of the smectite-illite transformation. However, a thin shale layer (9,179 to 9,182 ft, 2,798 to 2,799 m) near the base of the Frio 'A' reservoir is surrounded by a very indurated sandstone which contains spotty patches of authigenic kaolinite cement. The spotty zone is some 20 inches thick above the shale but only 4 inches thick below the shale, and is the best evidence for the introduction of fluids formed by clay dewatering which resulted in crystallization of authigenic kaolinite in the sandstones. Crystallization of abundant kaolinite in the adjacent sandstones has greatly reduced their reservoir quality.

Authigenic kaolinite is abundant in sandstones over the depth range 8,000 ft (2,438 m) to at least 17,700 ft (5,395 m) in Brazoria County (Loucks, Richmann, and Milliken, 1981; Ewing and others, 1983). In general the precipitation of kaolinite postdates the formation of quartz overgrowths and the subsequent leaching of calcite and formation of secondary porosity (Kaiser and Richmann, 1981). Major authigenic kaolinite began to crystallize in the Frio sandstones in Brazoria County around 100°C (212°F) (Loucks, Richmann, and Milliken, 1981). The smectite-illite transition in the shales begins at 90° to 100°C (194 to

212°F), which is similar to the temperature of major crystallization of authigenic kaolinite (Foscolos et al., 1976; Loucks, Richmann, and Milliken, 1981). The present temperature of the Frio 'A' sandstone at the Hitchcock N.E. field is around 101°C (215°F) indicating both that illite should have begun to form from smectite and that major authigenic kaolinite should have begun to crystallize.

Measured pH values (6.2-7.1) of Frio Formation waters in Brazoria County (Kharaka and others, 1979) indicate that the fluids lie within the chlorite and not kaolinite stability field, contradicting petrographic evidence (Kaiser and Richmann, 1981). The stability of these two minerals is controlled essentially by the pH and Mg-Fe log activity product of the fluids (Kaiser and Richmann, 1981). However, Kharaka and others (1979) have shown that pH values measured at well sites and wellhead temperatures are up to 2 pH units greater than the estimated (and probable) pH in the formation itself. Hence the measured pH values of 6.9-7.74 at the Huff A No. 1, Delee No. 1, Thompson No. 1, and Prets No. 1 wells (Kharaka and others, 1979; Randolph, 1985) probably represent an in situ pH in the formation of 5-6. Kaolinite is stable in formation waters with pH values from 5-6 in Brazoria County (Kaiser and Richmann, 1981), which explains its abundance in the Delee No. 1 core. The increased value of the measured pH compared to the true in situ value may result from dilution of the formation water by condensed water vapor produced with the natural gas (Kharaka and others, 1977). This is believed responsible for many of the reports of less saline than normal water in the geopressured zone (Kharaka and others, 1977).

The relative stability of feldspar versus kaolinite has been examined by Kaiser and Richmann (1981). In shallower hydropressured waters plagioclase is stable at temperatures less than 100°C, while kaolinite is stable relative to plagioclase under geopressured conditions. The fact that the Frio 'A' sandstone is some 2,000 ft (609 m) below the top of geopressure in the Hitchcock N.E. field in a zone with a geopressure gradient of 0.6 psi/ft

(fig. 2) is the probable explanation why there has been widespread replacement of feldspar by kaolin in this reservoir.

Shale Dewatering During Production

There is very little evidence presently available which can be used to demonstrate shale fluid flow (dewatering) during production. However, the formation water at the Phillips Prets No. 1 well has been analyzed on three occasions, eight years ago (Kharaka and others, 1977) and more recently by IGT and the University of Houston staff (Randolph, 1985). There is uncertainty about the quality of the early analyses and differences in the sampling points and procedures. Nevertheless the slight decrease in chloride ion concentration of about 5.5 to 8.7% may indicate shale dewatering (Table 5). Fowler, using 94 water analyses from Frio sandstones in the Chocolate Bayou field, has calculated the percentage change in chloride ion production over long periods of time, which is a result of dilution of the original formation waters by waters squeezed out of the shales adjacent to the aquifers with the declining pressures in the reservoir sandstones. Reductions in chloride ion concentration varied from 0.5 to 42.3% in ten of the reservoirs in which shale dewatering is believed to have occurred with a mean value of some 18.5% (Fowler, 1978). The Frio 'A' sandstone showed a 12.4% reduction in salinity in the Chocolate Bayou field over a production period of some 18 years. The fact that the Hitchcock N.E. field has produced for some 25 years (Anderson and others, 1984) indicates that this order of variation in the chloride ion concentration is to be expected if major shale dewatering did occur due to pressure drawdown. To more accurately investigate the effects of shale dewatering during the co-production of the Hitchcock N.E. field it is proposed that the time dependent variation of the elemental composition of brine produced at the Delee No. 1 well be measured. This should be done over a long time interval and the analyses made periodically to see if there is a systematic change in the concentrations of major, trace, and rare-earth element concentrations. These concentrations can be related to the

Table 5. Brine Analyses Results, Phillips Prets No. 1 Well.

	Kharaka and others, 1977	Southern Pet. Lab. Inc., 1982	University of Houston, 1984	I.G.T., 1985
Sampling Point	?	Brine Tank	Prets Separator	Prets Separator
TDS	44,600	38,700		44,000
Li	4.0			3.56
Na	17,000	14,400		16,800
K	160			120
Rb	0.40			
Ca	470	511		420
Mg	85	79		70.4
Sr	35			37.0
Ba	16	<1		16.8
Fe	0.1	15		11.3
Mn	0.4			0.5
B	41			
NH_3	17.0			15.0
H_2S	0.62			
HCO_3	643	687		
CH_3COO	750			
Cl	25,200	23,000	25,000	23,800
Br	25			
I	15			
SO_4	34	20		10.4
SiO_2	65			64
pH	6.9			7.74
δD	-14.5 SMOW			

elemental concentrations in ml/L

effects of shale dewatering or to water introduction from deeper levels (water drive from a large aquifer or leaky faults). It may be possible by measuring the amount of elemental variation to estimate the volume of water being added by shale dewatering and thus estimate the reduction in pressure depletion of the reservoir during rapid pressure drawdown.

The content of iron in the formation fluids shows a large increase from 0.1 to 11 to 15 mg/L in the Prets No. 1 well when the earlier and more recent analyses are compared (Table 5). This iron may be derived from oxidation of casing in the production wells over the long period of production (25 years) of the Hitchcock N.E. field. However, the data available only apply to the last 8 years of production.

The variation of elemental abundance, compounds, and isotopes has been plotted against both depth and chlorine content for wells in Brazoria and Galveston Counties. Most elements show a trend with depth with values from the Prets No. 1 well tending to plot on the opposite end of the trend compared to those from the Pleasant Bayou geopressured-geothermal wells (fig. 19) (Kharaka and others, 1977).

The δD (Deuterium/Hydrogen) value becomes depleted with depth in Brazoria and Galveston Counties (fig. 20) (Kharaka and others, 1977) and the variation in δD over time in the Delee No. 1 well should indicate whether shale dewatering is occurring or the fluids are more deeply sourced. A similar but larger variation is shown by the concentration of short chain aliphatic acids (C_2-C_5) (fig. 21) (Kharaka and others, 1977).

Shale Pyrolysis Data

Forty shale samples from the Anahuac and Frio Formations in the Delee No. 1 well were subjected to total organic carbon and Rock-Eval pyrolysis analyses by Geochem Laboratories, Inc.

The total organic carbon (TOC) in shales averaged 0.35% (range 0.17-1.06), which indicates that these shales are very poor hydrocarbon source rocks (Table 6a and b). One

Table 6a.

RESULTS OF ROCK-EVAL PYROLYSIS

GeoChem Sample No.	Depth Interval (Feet)	Tmax (c)	S_1 (mg/g)	S_2 (mg/g)	S_3 (mg/g)	PI	PC*	T.O.C. (wt.%)	Hydrogen Index	Oxygen Index
3013-001	6758	409	0.02	0.30	1.41	0.06	0.02	0.85	35	165
3013-002	6863	430	0.02	0.26	1.42	0.07	0.02	1.06	24	133
3013-003	6887	416	0.01	0.05	0.48	0.17	0.00	0.36	13	133
3013-004	7020	391*	0.02	0.07	0.48	0.25	0.00	0.28	25	171
3013-005	7113	386*	0.01	0.11	0.57	0.08	0.01	0.47	23	121
3013-006	7176	415*	0.01	0.09	0.53	0.10	0.00	0.35	25	151
3013-007	7216	375*	0.02	0.09	0.79	0.20	0.00	0.34	26	232
3013-008	7262	405*	0.02	0.08	0.42	0.20	0.00	0.32	25	131
3013-009	7294	354*	0.00	0.06	0.45	0.00	0.00	0.34	17	132
3013-010	7392	410*	0.02	0.08	0.44	0.20	0.00	0.33	24	133
3013-011	7534	354*	0.03	0.07	0.36	0.30	0.00	0.27	25	133
3013-012	7679	395*	0.01	0.14	0.50	0.07	0.01	0.39	35	128
3013-013	7858	394*	0.01	0.07	0.35	0.12	0.00	0.26	26	134
3013-014	7990	377*	0.00	0.06	0.36	0.00	0.00	0.27	22	133
3013-015	8126	415*	0.01	0.07	0.32	0.12	0.00	0.27	25	118
3013-016	8304	413	0.02	0.09	0.28	0.20	0.00	0.30	30	93
3013-017	8432	385*	0.03	0.10	0.36	0.25	0.01	0.30	33	120
3013-018	8602	409*	0.02	0.08	0.22	0.20	0.00	0.27	29	81
3013-019	8759	406*	0.02	0.09	0.21	0.20	0.00	0.30	30	70
3013-020	8913	415*	0.02	0.14	0.48	0.12	0.01	0.64	21	75
3013-021	8999	360*	0.01	0.07	0.28	0.12	0.00	0.31	22	90
3013-022	9070	337*	0.03	0.08	0.24	0.30	0.00	0.30	26	80
3013-023	9083.5	423*	0.03	0.07	0.25	0.30	0.00	0.20	35	125
3013-024	9092	376*	0.02	0.06	0.20	0.25	0.00	0.23	26	86
3013-025	9099'5.5"	323*	0.02	0.03	0.14	0.50	0.00	0.17	17	82
3013-026	9100	329*	0.02	0.08	0.28	0.20	0.00	0.22	36	127
3013-027	9100 6"	314*	0.02	0.05	0.17	0.33	0.00	0.17	29	100
3013-028	9100 7.25"	299*	0.02	0.07	0.25	0.25	0.00	0.17	41	147
3013-029	9101	318*	0.02	0.09	0.28	0.20	0.00	0.21	42	133

*The S2 value, or quantity of kerogen pyrolyzed to bitumen, is insufficient to produce a valid Tmax

T.O.C. = Total organic carbon, wt.%
S1 = Free hydrocarbons, mg HC/g of rock
S2 = Residual hydrocarbon potential (mg HC/g or rock)
S_3 = CO2 produced from kerogen pyrolysis (mg CO2/g of rock)
PC* = 0.083 (S1 + S2)
Hydrogen Index = mg HC/g organic carbon
Oxygen Index = mg CO2/g organic carbon
PI = S1/S1 + S2
Tmax = Temperature Index, degrees C.

Table 6b.

RESULTS OF ROCK-EVAL PYROLYSIS

GeoChem Sample No.	Depth Interval (Feet)	Tmax (c)	S_1 (mg/g)	S_2 (mg/g)	S_3 (mg/g)	PI	PC*	T.O.C. (wt.%)	Hydrogen Index	Oxygen Index
3013-030	9104 5"	421	0.04	0.40	0.38	0.09	0.03	0.58	68	65
3013-031	9179 11"	403*	0.02	0.07	0.20	0.25	0.00	0.21	33	95
3013-032	9194 3"	425	0.03	0.20	0.19	0.14	0.01	0.35	57	54
3013-033	9262	423	0.01	0.21	0.49	0.05	0.01	0.44	47	111
3013-034	9288	416	0.01	0.15	0.32	0.06	0.01	0.37	40	86
3013-035	9302	401*	0.01	0.12	0.35	0.08	0.01	0.34	35	102
3013-036	9340	302*	0.01	0.03	0.44	0.25	0.00	0.20	15	220
3013-037	9351	336*	0.01	0.10	0.37	0.10	0.00	0.27	37	137
3013-038	9367-9371	377*	0.03	0.29	0.30	0.09	0.02	0.43	67	69
3013-039	9370-9392	333	0.27	0.76	0.47	0.26	0.08	0.43	176	109
3013-040	9392-9402	343	0.02	0.15	0.31	0.12	0.01	0.29	51	106

*The S2 value, or quantity of kerogen pyrolyzed to bitumen, is insufficient to produce a valid Tmax.

T.O.C. = Total organic carbon, wt.%
S1 = Free hydrocarbons, mg HC/g of rock
S2 = Residual hydrocarbon potential (mg HC/g or rock)
S_3 = CO_2 produced from kerogen pyrolysis (mg CO_2/g of rock)
PC* = 0.083 (S1 + S2)
Hydrogen Index = mg HC/g organic carbon
Oxygen Index = mg CO_2/g organic carbon
PI = S1/S1 + S2
Tmax = Temperature Index, degrees C.

sample from 6,863 ft (2092 m) had a TOC of 1.06% while a thin coaly shale within the top of the Frio 'A' sandstone at 9,104 ft 5 inches contained 0.58% TOC. Total organic carbon contents of Frio shales beneath the Frio 'A' sandstone are variable (0.20 to 0.44% TOC) but on average are lean (mean = 0.33% TOC).

Rock-Eval pyrolysis is a technique used to evaluate the maturity of source rocks, a procedure that involves heating a shale sample in the absence of oxygen to break down large hydrocarbon molecules into smaller ones (Milner, 1982; Dutton, in press). Dutton (in press) has outlined the pyrolysis procedure. As the temperature is gradually increased, the sample will first give off hydrocarbons (S1) that are already present in the rock either in a free or adsorbed state (Tissot and Welte, 1978). When the temperature is raised further, kerogen in the sample will generate new hydrocarbons (S2), imitating in the laboratory the natural process of hydrocarbon generation. Finally, the CO_2 that is generated during pyrolysis is measured (S3) as an indication of the type of kerogen in the sample, whether it is humic (oxygen rich) or sapropelic (hydrogen-rich) (Hunt, 1979). Thermal maturity is measured by comparing the temperature of maximum evolution of thermally-cracked hydrocarbons (T-max°C) versus the proportion of free hydrocarbons (Sl) in the sample compared to total hydrocarbons (Sl + S2), that is, T-max°C versus S1/(S1 + S2). An example of the various peaks and a key for interpreting the pyrolysis data are given in figure 22 (Dow, 1981).

The source potential (values of S2) for the shales in the Delee No. 1 well averages 0.13 mg/g (range .03-.76 mg/g), well below the 2.5 mg/g upper limit for poor source potential (table 6a and b, fig. 22). The thin coaly shale within the top of the Frio 'A' sandstone has a slightly better source potential of 0.4 mg/g while deeper Frio shales at 9,370-9,392 ft have source potentials of 0.76 mg/g. The source potential values indicate that it is extremely unlikely that the condensate in the Frio 'A' reservoir could have been been derived from either the Anahuac or Frio shales.

The ratio of S2/S3 provides a general indication of kerogen quality (type) and reveals whether oil or gas is likely to be generated (Dow, 1981). Dry gas generating kerogens have S2/S3 values less than 2.5. S2/S3 values for the Delee No. 1 well average 0.35 (range 0.1-1.6), which suggests that the kerogen is a poor source even for dry gas (fig. 22).

The hydrogen and oxygen index data for shales in the Delee well indicate that the kerogen is of type III, consisting essentially of woody and coaly material (fig. 23). The T-max°C values for all these samples are less than 435°C, indicating that this lignitic material is immature (fig. 24). However, many of the samples contained such a small quantity of organic matter (kerogen) that it was insufficient to produce a valid T-max°C.

$\delta^{13}C$ values have been estimated for the aromatics and the saturates in oil from the Prets No. 1 well by Coastal Science Laboratories, Inc., Austin, Texas. Calculations of the canonical variable from these data and pristane-phytane ratios (figs. 25 and 26) indicate that the Prets No. 1 oil is correctly classified as a non-waxy oil sourced from marine organic matter. This is in contrast to the terrigenous nature of the kerogen in the Anahuac and Frio shales and implies that these oils have been sourced from other (deeper) formations.

CONCLUSIONS

The high porosity (±30%) and permeability (±1,000 md, 0.99 μm^2) of the Frio 'A' reservoir in the Hitchcock N.E. field are largely the result of deposition in a distributary-mouth-bar complex. As a consequence of extensive marine reworking the lateral extent of this sandstone will allow free access to water influx from the southwest extension of this aquifer.

The location of the Hitchcock N.E. field on the northeast flank of the large faulted Frio 'A' aquifer isolated to the north and south by northeast trending fault systems has bearing on the best location of guard wells below the gas-water contact to control water influx.

Minor faults which dissect the Hitchcock N.E. field may locally isolate certain parts of the pay zone where shale or permeability breaks are present. Knowledge of the position and extent of these zones will also control the best placement of guard wells. However, reservoir modeling suggests that the faults are not sealing over the fairly long time frame of pressure drawdown during co-production.

Vitrinite reflectance at the DOW-D.O.E. Pleasant Bayou wells, supported by hydrocarbon maturation and isotope data, indicates that the upper Frio was subjected to an extended period of hot, extremely saline, basinal-fluid flow. This fluid flow appears to have introduced hydrocarbons into these sandstones, caused albitization of the feldspars, and formed the carbonate cements.

Elemental composition data for Anahuac and Frio shales at the Delee No. 1 well indicate that they have a consistent illite-smectite composition and no clear evidence was found for shale dewatering. However, spotty indurated authigenic kaolinite zones, developed in the Frio 'A' sandstone adjacent to thin shale units, probably result from fluids emitted from the shales. Slight reduction in salinity during production at the Prets No. 1 well may be evidence for contemporaneous dewatering of shales.

Shale pyrolysis data indicate that the Anahuac and Frio shales contain coaly or woody kerogen of very poor hydrocarbon source quality. Furthermore, all the samples appear immature. In contrast isotope data indicate that the Prets No. 1 condensates are derived from marine organic matter further supporting a deep source for these fluids.

IMMEDIATE RESEARCH PLANS

The initial part of the effort by the Bureau of Economic Geology will be to screen previously unidentified candidate reservoirs for enhanced gas recovery during the next contract period. Work on this project has begun. In the process of identifying these reservoirs we will refine previously used criteria and will develop new criteria that can be

applied in selecting potential co-production reservoirs. The best 10 (±2) fields will be selected for detailed reservoir evaluation. These data will be made available to groups conducting reservoir simulation that are contracted to the Gas Research Institute. They will determine the total reservoir initial volume and estimate the recoverable gas reserves using the co-production of gas and water pressure drawdown enhancement procedure.

Work on the Delee No. 1 well will be continued but on a reduced scale. The Shale Frio 'A' sandstone boundary will be examined using scanning electron microscopy and petrographic studies. These data bear on fluid migration and shale dewatering.

Gas chromatography/mass spectrometry and isotope analyses of hydrocarbons and formation fluids from the Prets and Delee wells are still to be received from Geochem Labs., Inc., and Coastal Science Labs., Inc., respectively. These data will be statistically compared by computer with hydrocarbon extract data from shales from the Pleasant Bayou test wells for the entire Frio, Anahuac, and Miocene sequence (16,500 ft in total). This will attempt to locate the source of the hydrocarbons.

It is proposed that detailed major, trace, and rare-earth analyses be conducted periodically on produced fluids from the Delee No. 1 well as well as the shales surrounding the Frio 'A' sandstone. These data should indicate the amount of shale dewatering that is occurring as a result of the pressure drawdown during the co-production of gas and water.

ACKNOWLEDGMENTS

We wish to thank R. A. Morton, W. E. Galloway, W. R. Kaiser, and N. Tyler for valuable discussions and assistance in the project; Z. S. Lin for general engineering concepts. We gratefully acknowledge assistance given by L. L. Anderson, K. P. Peterson, and W. A. Parisi of Eaton Industries of Houston, Inc. XRD and ICP analyses were done at the Mineral Studies Laboratory by Steven W. Tweedy under the direction of David W. Koppenaal. The text was typed by Dorothy C. Johnson under the direction of Lucille C. Harrell. Illustrations were drafted by Tom Byrd, Annie Kubert, Jamie McClelland,

Nan Minchow, and Linda Morace under the direction of Richard L. Dillon. Funding for this research was provided by the Gas Research Institute under contract no. 5084-212-0924. The manuscript was reviewed by R. J. Finley.

REFERENCES

Anderson, L. L., Peterson, K. P., and Parisi, W. A., 1984, Enhanced production from a slightly geopressured water-drive gas condensate field: Presented at 1984 SPE/DOE/GRI Unconventional Gas Recovery Symposium, Pittsburgh, PA, p. 341-344.

Bebout, D. G., Loucks, R. G., and Gregory, A. R., 1978, Frio sandstone reservoirs in the deep subsurface along the Texas Gulf Coast: The University of Texas at Austin, Bureau of Economic Geology Report of Investigations 91, 92 p.

Blatt, H., Middleton, G., and Murray, R., 1972, Origin of sedimentary rocks: Englewood Cliffs, New Jersey, Prentice-Hall, 634 p.

Boles, J. R., and Franks, S. G., 1979, Clay diagenesis in Wilcox sandstones of southwest Texas, implications of smectite diagenesis on sandstone cementation: Journal of Sedimentary Petrology, v. 49, no. 1, p. 55-70.

Brown, S. W., 1980, Hydrocarbon source facies analysis, Department of Energy and General Crude Oil Company Pleasant Bayou No. 1 and 2 wells, Brazoria County, Texas, in Proceedings, Fourth Conference on Geopressured Geothermal Energy: The University of Texas at Austin, p. 132-152.

Burst, J. F., 1969, Diagenesis of Gulf Coast clayey sediments and its possible relationship to petroleum migration: American Association of Petroleum Geologists Bulletin, v. 53, no. 1, p. 73-93.

Coleman, J. M., and Prior, D. B., 1980, Deltaic sand bodies. A 1980 short course: American Association of Petroleum Geologists Continuing Education Course Note Series 15, AAPG, Tulsa, OK, 171 p.

Collins, A. G., 1975, Geochemistry of oil field waters: New York, Elsevier, 496 p.

Deer, W. A., Howie, R. A., and Zussman, J., 1969, An introduction to the rock-forming minerals: London, Longmans, 528 p.

Dorfman, M. H., 1982, The outlook for geopressured/geothermal energy and associated natural gas: Journal of Petroleum Technology, p. 1915-1919.

Dow, W. G., and Page, M. M., 1981, Geochemical evaluation of the Cameron Park and Development Company #1, Cameron County, Texas: Report No. 284 prepared for The University of Texas at Austin, Bureau of Economic Geology, by Robertson Research (U.S.), Inc., 36 p.

Dutton, S. P., in press, Organic geochemistry of the Pennsylvanian and Lower Permian, Palo Duro Basin, Texas: The University of Texas at Austin, Bureau of Economic Geology Report.

Ewing, T. E., Light, M. P. R., and Tyler, N., 1984, In T. E. Ewing, N. Tyler, R. A. Morton, and M. P. R. Light. Consolidation of geologic studies of geopressured geothermal resources of Texas: The University of Texas at Austin, Bureau of Economic Geology, report prepared for the U.S. Department of Energy, Contract No. DE-AC08-79ET27111, 90-142.

Foscolos, A. E., 1984, Diagenesis. Catagenesis of Argillaceous Sedimentary Rocks. Geoscience Canada, v. 11, no. 2, p. 67-75.

Foscolos, A. E., and Powell, T. G., 1980, Mineralogical and geochemical transformation of clays during burial catagenesis and their relation to oil generation: Canadian Society of Petroleum Geologists, Memoir 6, p. 153-172.

Galloway, W. E., Hobday, D. K., and Magara, K., 1982, Frio Formation of the Texas Gulf Coast Basin - depositional systems, structural framework, and hydrocarbon origin, migration, distribution and exploration potential. The University of Texas at Austin, Bureau of Economic Geology Report of Investigations 122, 78 p.

Gregory, A. R., Lin, Z. S., Reed, R. S., Morton, R. A., and Rogers, L. A., 1983, Watered-out gas reservoirs profitable via enhanced recovery. Oil and Gas Journal, v. 81, no. 11, p. 55-60.

Hinch, H. H., 1980, The nature of shales and the dynamics of hydrocarbon expulsion in the Gulf Coast tertiary section, in Roberts, W. H., and Cordell, R. J., eds., Problems in Petroleum Migration: American Association of Petroleum Geologists Studies in Geology, v. 10, p. 1-18.

Hower, J., Eslinger, E. V., Hower, M. E., and Perry, E. A., 1976, Mechanism of burial metamorphism of argillaceous sediment, 1.: mineralogical and chemical evidence: Geological Society of America Bulletin, v. 87, no. 5, p. 725-737.

Hunt, J. M., 1979, Petroleum geochemistry and geology: San Francisco, W. H. Freeman, 617 p.

Kaiser, W. R., and Richmann, D. L., 1981, Predicting diagenetic history and reservoir quality in the Frio Formation of Brazoria County, Texas, and Pleasant Bayou test wells, in Proceedings, Fifth Conference on Geopressured Geothermal Energy: The University of Texas at Austin, p. 67-74.

Kharaka, Y. K., Lies, M. S., Wright, V. A., and Carothers, W. W., 1979, Geochemistry of formation waters from Pleasant Bayou No. 2 well and adjacent areas in coastal Texas, in Proceedings, Fourth Conference on Geopressured Geothermal Energy: The University of Texas at Austin, p. 11-45.

Kharaka, Y. K., Callender, E., and Carothers, W. W., 1977, Geochemistry of geopressured-geothermal waters from the Texas Gulf Coast: in Meriwether, J. R., ed., Third geopressured-geothermal energy conference, University of Southwestern Louisiana, Lafayette, Louisiana, v. 1, G-121-G-165.

Lewis, C. R., and Rose, S. C., 1970, A theory relating high temperatures and overpressures: Journal of Petroleum Technology, v. 22, no. 1, p. 11-16.

Light, M. P. R., Ewing, T. E., and Tyler, N., (in prep.), Thermal history and hydrocarbon anomalies in the Frio Formation, Brazoria County, Texas--An indicator of fluid flow and geopressure history: The University of Texas at Austin, Bureau of Economic Geology, report prepared for the U.S. Department of Energy, Contract No. DE-AC08-79ET27111, 90-142.

Light, M. P. R., 1985, Maturity anomalies, fluid flow, and permeability preservation in Frio and Anahuac Formations, Upper Texas Gulf Coast (abs.): Annual convention of the American Association of Petroleum Geologists, New Orleans, Louisiana, March 24-27.

Loucks, R. G., Richmann, D. L., and Milliken, K. L., 1981, Factors controlling reservoir quality in Tertiary sandstones and their significance to geopressured geothermal production: The University of Texas at Austin, Bureau of Economic Geology Report of Investigations 111, 41 p.

Milliken, K. L., Land, L. S., and Loucks, R. G., 1981, History of burial diagenesis of determined from isotopic geochemistry, Frio Formation, Brazoria County, Texas: American Association of Petroleum Geologists Bulletin, v. 65, p. 1397-1413.

Milner, C. W. D., 1982, Geochemical analyses of sedimentary organic matter and interpretation of maturation and source potential, in How to assess maturation and paleotemperatures: Society of Economic Paleontologists and Mineralogists short course 7, p. 217-252.

Mooney, R. W., Keenan, A. G., and Wood, L. A., 1952, Adsorption of water vapor by montmorillonite. 1. Heat of desorption and application of BET theory: Journal of the American Chemical Society, v. 74, p. 1367-1371.

Morton, J. P., 1983, Age of clay diagenesis in the Oligocene Frio Formation, Texas Gulf Coast: The University of Texas at Austin, Ph. D. dissertation, 33 p.

Morton, R. A., Ewing, T. E., and Tyler, N., 1983, Continuity and internal properties of Gulf Coast sandstones and their implications for geopressured fluid production: The

University of Texas at Austin, Bureau of Economic Geology Report of Investigations 132, 70 p.

Nadeau, P. H., Wilson, M. J., McHardy, W. J., and Tait, J. M., 1984, Interstratified clays as fundamental particles: Science, v. 225, p. 923-925.

Powell, T. G., Foscolos, A. E., Gunther, P. R., and Snowdon, L. R., 1978, Diagenesis of organic matter and fine clay minerals: a comparative study: Geochimica et Cosmochimica Acta, v. 42, p. 1181-1197.

Pryor, W. A., 1973, Permeability-porosity patterns and variations in some Holocene sand bodies: American Association of Petroleum Geologists Bulletin 57, 162-189.

Randolph, P. L., 1985, Preliminary Hitchcock N.E. well and reservoir data April 1, 1985: Provisional report prepared for the Gas Research Institute by the Institute of Gas Technology, Chicago.

Reznikov, A. N., 1967, The geochemical conversion of oils and condensates in the zone of katagenesis: Geologiya Nefti i gaza, no. 5, p. 24-28.

Schoell, M., 1983, Genetic characterization of natural gases: The American Association of Petroleum Geologists Bulletin, v. 67, no. 12, p. 2225-2238.

Sofer, Z., 1984, Stable carbon isotope compositions of crude oils: application to source depositional environments and petroleum alteration: American Association of Petroleum Geologists Bulletin, v. 68, no. 1, p. 31-49.

Tissot, B. P., and Welte, D. H., 1978, Petroleum formation and occurrence: Berlin, Springer-Verlag, 538 p.

Tyler, N., Light, M. P. R., and Ewing, T. E., 1985, Saline fluid flow and hydrocarbon migration and maturation as related to geopressure, Frio Formation, Brazoria County, Texas (abs.): Sixth U.S. Gulf Coast Geopressured-Geothermal Energy Conference, The University of Texas at Austin, Texas, p. 11.

Waples, D. W., 1980, Time and temperature in petroleum formation: application of Lopatin's method to petroleum exploration: American Association of Petroleum Geologists Bulletin, v. 64, no. 6, p. 916-926.

Weres, O., Michel, M., Harnden, W., and Newton, A., 1984, Downhole sampling of geopressured gas wells: The University of California, Lawrence Berkeley Laboratory, report prepared for the Gas Research Institute, Contract No. 5081-212-0552, 53 p.

Young, A., Monaghan, P. H., and Schweisberger, R. T., 1977, Calculation of ages of hydrocarbons in oils--physical chemistry applied to petroleum geochemistry: American Association of Petroleum Geologists Bulletin, v. 61, no. 4, p. 573-600.

APPENDIX

APPENDIX

Detailed listing of Geochem Labs., Inc., analyses of hydrocarbons and shales from the Prets No. 1 and Delee No. 1 wells.

Sample Preparation

Routine preparation - sample handling - dry cuttings: includes inventory, sieving of samples to remove cavings, crushing and grinding, compositing, and packaging.

Source Rock Analyses

Total organic carbon and Rock-Eval pyrolysis analysis.

Crude Oil Characterization

C_4-C_7 detailed gasoline-range gas-chromatographic analysis.

C^{15+} liquid chromatographic separation, involves topping of less than C^{15+} fraction, deasphaltening and liquid chromatographic separation to isolate C^{15+} paraffin-naphthene (P-N) hydrocarbon, C^{15+} aromatic (AROM) hydrocarbon, and C^{15+} N-S-O nonhydrocarbon fractions.

Desulfurization of C^{15+} paraffin-naphthene (P-N) hydrocarbon and C^{15+} aromatic (AROM) hydrocarbon fractions.

Nickel-vanadium elemental analysis.

API gravity and specific gravity.

GC/MS/DS analysis of C^{15+} aromatic (AROM) hydrocarbon fraction of crude oil.

Saturate Terpane and Sterane Hydrocarbons - liquid chromatography to obtain C^{15+} paraffin-naphthene (P-N) hydrocarbon, C^{15+} aromatic (AROM) hydrocarbon, C^{15+} N-S-O nonhydrocarbon.

Molecular sieve removal of n-alkanes from C^{15+} paraffin-naphthene (P-N) hydrocarbons.

Re-isolation of n-alkanes from molecular sieves (not necessary for terpane/sterane studies).

GC/MS analysis of isolated fraction.

Monoaromatic steranes - liquid chromatography to obtain C^{15+} paraffin-naphthene hydrocarbon, C^{15+}aromatic (AROM) hydrocarbon, and C^{15+}N-S-O nonhydrocarbon resins.

Monoaromatic steranes - liquid chromatography to obtain 1, 2, and 3-ring aromatic compounds.

Monoaromatic steranes - GC/MS analysis of isolated monoaromatic fraction.

Crude Oil to Crude Oil correlation - Crude Oil to Source Rock correlation - Tier II similarity analysis, cluster analysis, and ordination. Comparison with shale extract data from Pleasant Bayou No. 1 well.

Gas chromatographic analysis (glass capillary column) of C^{15+} paraffin-naphthene (P-N) hydrocarbon.

List of isotope analyses conducted by Coastal Science Labs., Inc. on hydrocarbon and formation water samples from the Prets No. 1 and Delee No. 1 wells.

Isotopes	Sample
$\delta^{13}C$ and $\delta^{2}H$	methane
$\delta^{13}C$	gas component (C_2, C_3, C_4, C_5, CO_2)
$\delta^{13}C$	condensate
$\delta^{13}C$	chromatographic fractions
$\delta^{18}O$ and $\delta^{2}H$	water
silica gel column chromatography	condensate

DETAILED TABLES AND HISTOGRAMS OF ROBERTSON RESEARCH (U.S.), INC. REFLECTED LIGHT MICROSCOPY DATA FOR SHALES FROM THE DELEE NO. 1 WELL

REFLECTED LIGHT MICROSCOPY DATA

A sample of ground rock is treated successively with hydrochloric and hydrofluoric acids to concentrate the kerogen, freeze-dried, mounted in an epoxy plug, and polished. Kerogen type is identified with the aid of blue light fluorescence.

The visual kerogen analysis data table contains visual percentage estimates of each principle kerogen type and kerogen background fluorescence data. This data is also displayed on the histograms with relative amounts of solid bitumen and coked material.

The histograms show measured reflectance values of all vitrinite present and on all material with the visual appearance of vitrinite. Shaded values (marked with *) are those used to calculate the interpreted vitrinite reflectance maturities. Unshaded values are interpreted to be oxidized vitrinite, recycled vitrinite, or possibly misidentified material such as solid bitumen, pseudo-vitrinite, or semifusinite. When samples analysed contain no vitrinite, nonindigenous vitrinite or have an insufficient number of readings to allow a reliable maturity determination to be made, then the mean value for that sample is shown as N. D. (Not Determined). Alternate maturity calculations are possible on a few samples. The histograms are identified by a Robertson Research sequence number (RRUS No.) and depth or other notation.

ABBREVIATIONS USED IN VISUAL KEROGEN ANALYSIS DATA SHEET AND HISTOGRAMS

Am	:	Amorphous Kerogen
Ex	:	Exinite
Vit	:	Vitrinite
Inert	:	Inertinite
R_o	:	Vitrinite Reflectance Mean in Immersion Oil
Bkg Fl	:	Background Fluorescence

VISUAL KEROGEN ANALYSIS - REFLECTED LIGHT

DE LEE #1 - HITCHCOCK FIELD

Project No. : RRUS/845/T/844/7

SAMPLE IDENTIFICATION			REFLECT.	KEROGEN CHARACTERISTICS					TOC
RRUS	ID / DEPTH	(Feet)	Ro %	Am%	Ex%	Vit%	Inert%	Fluor	%
1	CTGS.	6758.0	0.39	5	10	65	20	None	----
2	CTGS.	6887.0	0.37	25	10	60	5	Low	----
3	CTGS.	7020.0	0.38	20	10	30	10	Low	----
4	CTGS.	7110.0	0.44	25	5	55	15	Low	----
5	CTGS.	7176.0	0.44	20	5	60	15	Med	----
6	CTGS.	7216.0	0.41	55	5	30	10	Med	----
7	CTGS.	7262.0	0.49	50	5	30	15	High	----
8	CTGS.	7392.0	0.46	65	5	20	10	High	----
9	CTGS.	7534.0	0.46	35	10	40	15	High	----
10	CTGS.	7677.0	0.51	60	5	30	5	Med	----
11	CTGS.	7858.0	0.49	35	5	50	10	Med	----
12	CTGS.	7990.0	0.58	70	5	20	tr	Med	----
13	CTGS.	8126.0	0.52	80	0	10	10	Med	----
14	CTGS.	8304.0	0.47	80	0	5	15	Med	----
15	CTGS.	8429.0	0.57	55	15	20	10	Med	----
16	CTGS.	8602.0	0.57	70	50	15	10	Med	----
17	CTGS.	8759.0	0.58	75	0	15	10	Low	----
18	CTGS.	8913.0	0.65	55	5	30	10	Low	----
19	CORE	9070.0	0.68	60	0	30	10	Low	----
20	CORE	9083.0	0.66	45	5	40	10	Low	----
21	CORE	9092.0	0.67	30	0	65	5	None	----
22	CORE	9099.0	0.64	25	0	65	10	Low	----
23	CORE	9100.0	0.70	20	10	60	10	Med	----
24	CORE	9100.5	0.64	55	10	30	5	Low	----
25	CORE	9100.0	0.59	60	5	15	20	None	----
26	CORE	9100.8	0.64	45	15	30	10	Low	----
27	CORE	9101.0	0.70	75	0	15	10	Low	----
28	CORE	9103.3	0.66	85	0	10	5	Med	----
29	CORE	9104.5	0.56	40	5	50	5	Low	----
30	CORE	9125.0	0.58	55	tr	35	10	Low	----
31	CORE	9141.0	----	95	0	5	tr	Med	----
32	CORE	9149.0	----	90	0	5	5	Low	----
33	CORE	9167.5	----	90	0	5	5	Low	----
34	CORE	9179.9	0.73	45	0	35	20	Low	----
35	CORE	9194.3	0.60	35	5	50	10	Low	----
36	CORE	9262.0	0.63	45	10	35	10	Low	----
37	CTGS.	9302.0	0.58	40	15	35	10	Med	----
38	CTGS.	9340.0	0.60	30	5	50	15	Low	----
39	CTGS.	9367.0	----	40	5	40	15	Med	----
40	CTGS.	9392.0	----	45	5	40	10	None	----

DE LEE #1 - HITCHCOCK FIELD

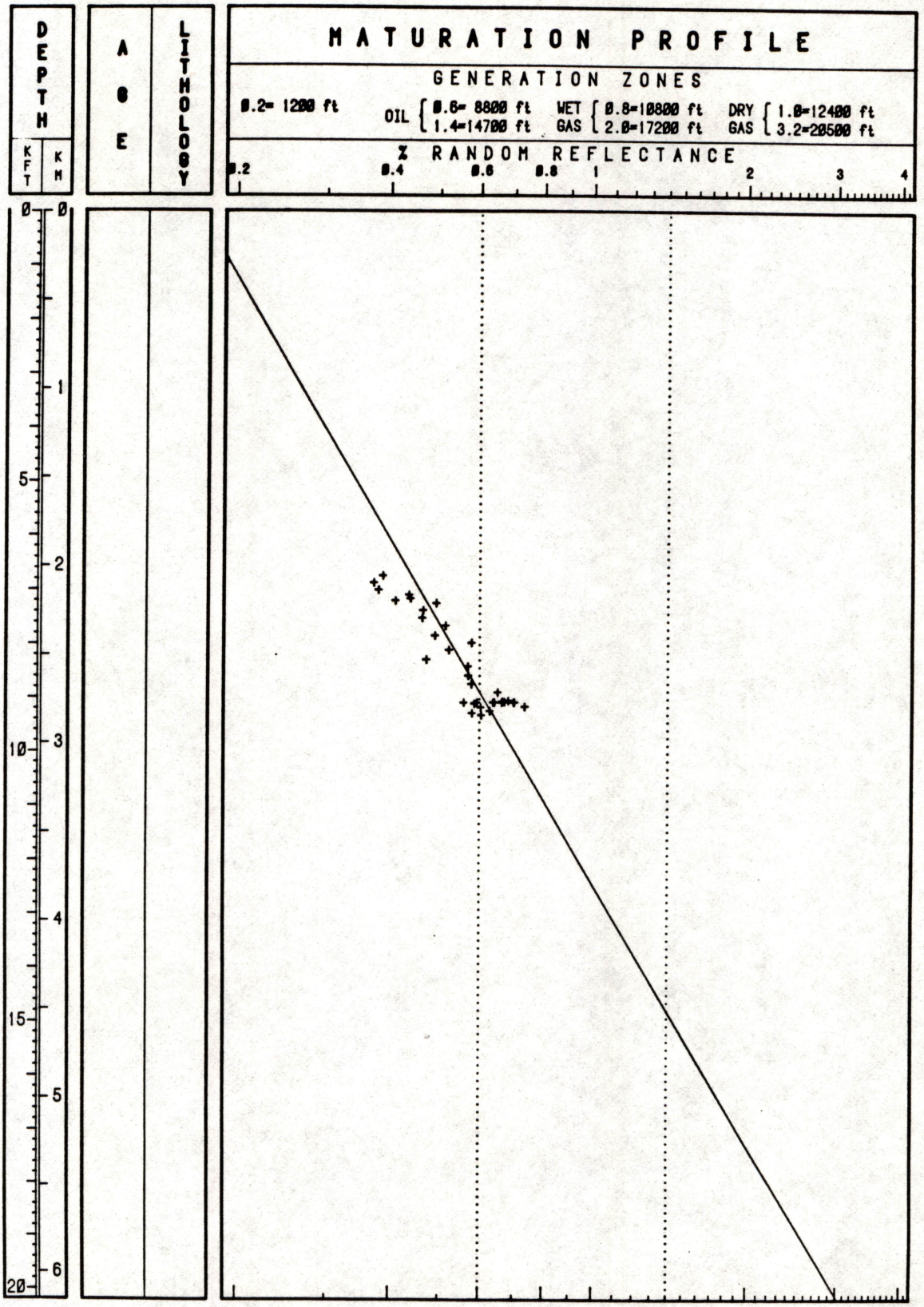

MATURATION PROFILE, BASED ON VITRINITE REFLECTANCE DATA

DE LEE #1 - HITCHCOCK FIELD

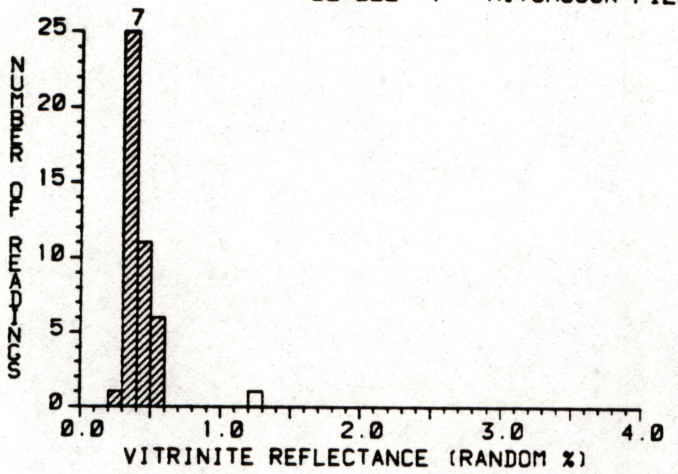

RRUS No. : 1
ID : CTGS.

DEPTH : 6758.0 Ft
: 2059.8 M

* = Ro MATURITY

VALUES : 50

MEAN : 0.39
STD DEV : 0.07
MEDIAN : 0.38
MODE : 0.35

HISTOGRAM:
Range: 0- 4%
Increment: 0.10%

ORDERED REFLECTANCE VALUES:

*0.25	*0.32	*0.36	*0.38	*0.47	1.20
*0.30	*0.32	*0.36	*0.39	*0.47	
*0.30	*0.33	*0.36	*0.39	*0.48	
*0.30	*0.33	*0.36	*0.40	*0.48	
*0.30	*0.33	*0.37	*0.40	*0.50	
*0.31	*0.33	*0.38	*0.44	*0.51	
*0.31	*0.34	*0.38	*0.44	*0.51	
*0.31	*0.34	*0.38	*0.45	*0.52	
*0.31	*0.36	*0.38	*0.46	*0.55	
*0.32	*0.36	*0.38	*0.47	*0.56	

KEROGEN DESCRIPTION

Amorphous	:	5 %
Exinite	:	10 %
Vitrinite	:	65 %
Inertinite	:	20 %
Back Fluor	:	None
Bitumen	:	None
Coke	:	tr

DE LEE #1 - HITCHCOCK FIELD

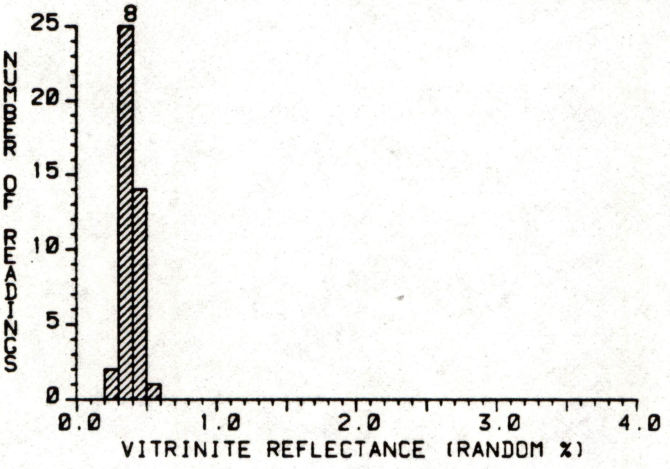

RRUS No. : 2
ID : CTGS.

DEPTH : 6887.0 Ft
: 2099.2 M

* = Ro MATURITY

VALUES : 50

MEAN : 0.37
STD DEV : 0.05
MEDIAN : 0.37
MODE : 0.35

HISTOGRAM:
Range: 0- 4%
Increment: 0.10%

ORDERED REFLECTANCE VALUES:

*0.26	*0.33	*0.35	*0.38	*0.41
*0.29	*0.34	*0.35	*0.39	*0.42
*0.30	*0.34	*0.35	*0.39	*0.42
*0.30	*0.34	*0.36	*0.39	*0.44
*0.31	*0.34	*0.37	*0.39	*0.45
*0.31	*0.34	*0.37	*0.40	*0.45
*0.31	*0.34	*0.37	*0.40	*0.46
*0.32	*0.34	*0.37	*0.40	*0.47
*0.33	*0.35	*0.38	*0.40	*0.49
*0.33	*0.35	*0.38	*0.40	*0.51

KEROGEN DESCRIPTION

Amorphous	:	25 %
Exinite	:	10 %
Vitrinite	:	60 %
Inertinite	:	5 %
Back Fluor	:	Low
Bitumen	:	None
Coke	:	None

DE LEE #1 - HITCHCOCK FIELD

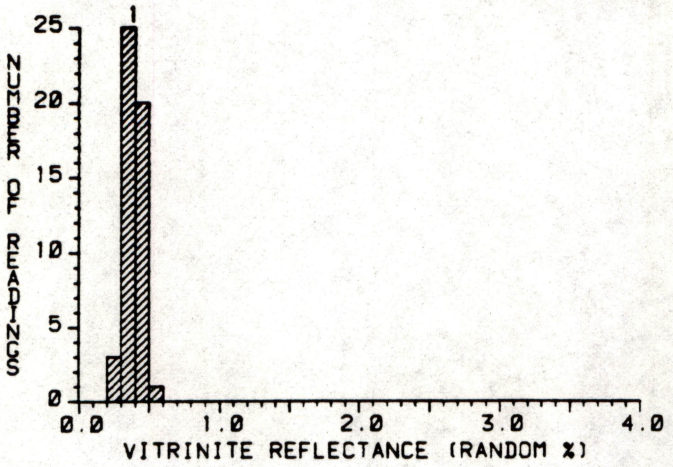

RRUS No. : 3
ID : CTGS.

DEPTH : 7020.0 Ft
: 2139.7 M

* = Ro MATURITY

VALUES : 50

MEAN : 0.38
STD DEV : 0.06
MEDIAN : 0.38
MODE : 0.35

HISTOGRAM:
Range: 0- 4%
Increment: 0.10%

ORDERED REFLECTANCE VALUES:

*0.26	*0.33	*0.37	*0.40	*0.43
*0.27	*0.33	*0.37	*0.40	*0.43
*0.28	*0.33	*0.37	*0.40	*0.44
*0.30	*0.33	*0.37	*0.40	*0.45
*0.30	*0.35	*0.38	*0.41	*0.45
*0.31	*0.35	*0.38	*0.41	*0.46
*0.31	*0.35	*0.39	*0.41	*0.46
*0.32	*0.36	*0.39	*0.42	*0.47
*0.33	*0.36	*0.39	*0.43	*0.49
*0.33	*0.36	*0.40	*0.43	*0.52

KEROGEN DESCRIPTION

Amorphous : 20 %
Exinite : 10 %
Vitrinite : 30 %
Inertinite : 10 %

Back Fluor : Low
Bitumen : None
Coke : None

DE LEE #1 - HITCHCOCK FIELD

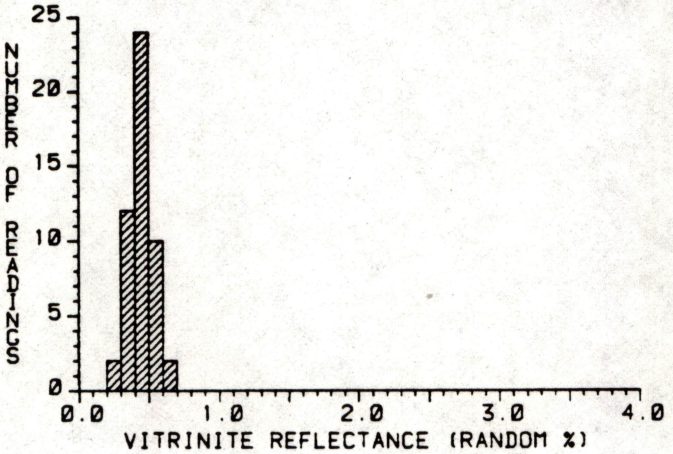

RRUS No. : 4
ID : CTGS.

DEPTH : 7110.0 Ft
: 2167.1 M

* = Ro MATURITY

VALUES : 50

MEAN : 0.44
STD DEV : 0.08
MEDIAN : 0.43
MODE : 0.45

HISTOGRAM:
Range: 0- 4%
Increment: 0.10%

ORDERED REFLECTANCE VALUES:

*0.28	*0.38	*0.42	*0.45	*0.52
*0.29	*0.38	*0.42	*0.45	*0.52
*0.31	*0.38	*0.42	*0.45	*0.52
*0.33	*0.39	*0.42	*0.46	*0.52
*0.33	*0.40	*0.43	*0.47	*0.53
*0.34	*0.40	*0.43	*0.47	*0.53
*0.34	*0.40	*0.44	*0.48	*0.56
*0.35	*0.41	*0.44	*0.48	*0.57
*0.36	*0.41	*0.44	*0.50	*0.61
*0.37	*0.41	*0.45	*0.50	*0.62

KEROGEN DESCRIPTION

Amorphous : 25 %
Exinite : 5 %
Vitrinite : 55 %
Inertinite : 15 %

Back Fluor : Low
Bitumen : None
Coke : None

DE LEE #1 - HITCHCOCK FIELD

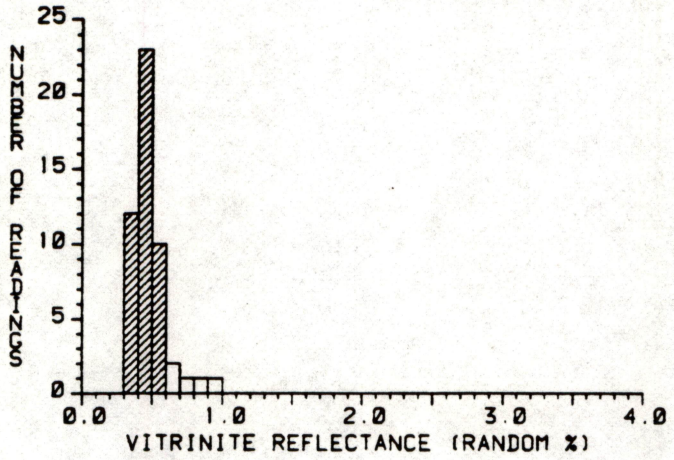

RRUS No. : 5

DEPTH : 7176.0 Ft
: 2187.2 M

* = Ro MATURITY

# VALUES	:	45
MEAN	:	0.44
STD DEV	:	0.06
MEDIAN	:	0.44
MODE	:	0.45

HISTOGRAM:
Range: 0- 4%
Increment: 0.10%

ORDERED REFLECTANCE VALUES:

*0.30	*0.39	*0.44	*0.45	*0.53
*0.30	*0.39	*0.44	*0.46	*0.53
*0.33	*0.41	*0.44	*0.48	*0.53
*0.33	*0.41	*0.44	*0.48	*0.56
*0.35	*0.41	*0.44	*0.49	*0.57
*0.37	*0.42	*0.45	*0.50	0.64
*0.38	*0.43	*0.45	*0.50	0.65
*0.38	*0.43	*0.45	*0.50	0.72
*0.38	*0.43	*0.45	*0.52	0.86
*0.38	*0.44	*0.45	*0.52	0.95

KEROGEN DESCRIPTION

Amorphous	:	20 %
Exinite	:	5 %
Vitrinite	:	60 %
Inertinite	:	15 %
Back Fluor	:	Med
Bitumen	:	tr
Coke	:	None

DE LEE #1 - HITCHCOCK FIELD

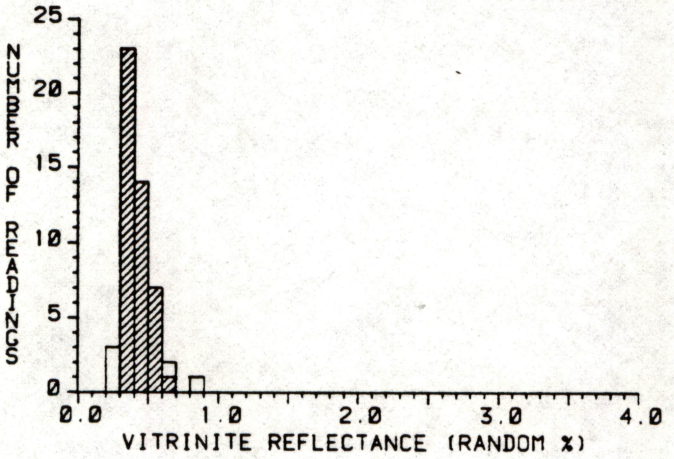

RRUS No. : 6
ID : CTGS.

DEPTH : 7216.0 Ft
: 2199.4 M

* = Ro MATURITY

# VALUES	:	45
MEAN	:	0.41
STD DEV	:	0.08
MEDIAN	:	0.39
MODE	:	0.35

HISTOGRAM:
Range: 0- 4%
Increment: 0.10%

ORDERED REFLECTANCE VALUES:

0.25	*0.33	*0.38	*0.41	*0.50
0.28	*0.34	*0.38	*0.41	*0.53
0.28	*0.34	*0.38	*0.43	*0.53
*0.30	*0.35	*0.39	*0.44	*0.54
*0.30	*0.35	*0.39	*0.44	*0.54
*0.30	*0.36	*0.39	*0.44	*0.54
*0.31	*0.37	*0.40	*0.45	*0.59
*0.32	*0.37	*0.40	*0.45	*0.62
*0.33	*0.37	*0.40	*0.46	0.67
*0.33	*0.38	*0.40	*0.46	0.88

KEROGEN DESCRIPTION

Amorphous	:	55 %
Exinite	:	5 %
Vitrinite	:	30 %
Inertinite	:	10 %
Back Fluor	:	Med
Bitumen	:	tr
Coke	:	None

DE LEE #1 - HITCHCOCK FIELD

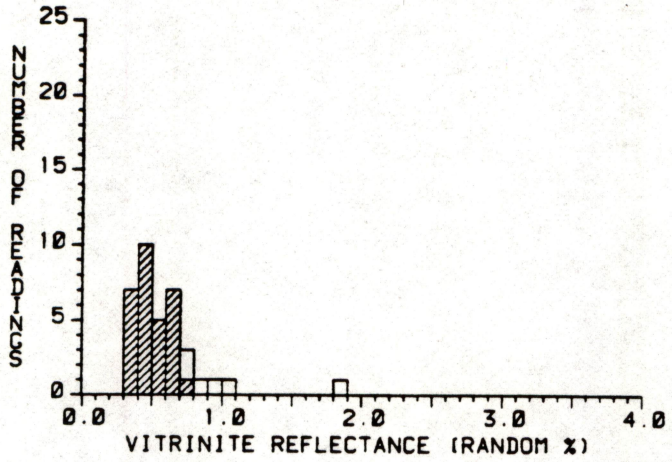

RRUS No. : 7
ID : CTGS.

DEPTH : 7262.0 Ft
: 2213.5 M

* = Ro MATURITY

VALUES : 30

MEAN : 0.49
STD DEV : 0.11
MEDIAN : 0.47
MODE : 0.45

HISTOGRAM:
Range: 0- 4%
Increment: 0.10%

ORDERED REFLECTANCE VALUES:

*0.32	*0.42	*0.52	0.75
*0.34	*0.43	*0.54	0.79
*0.36	*0.44	*0.62	0.87
*0.37	*0.45	*0.62	0.91
*0.39	*0.46	*0.63	1.00
*0.39	*0.47	*0.64	1.83
*0.39	*0.49	*0.67	
*0.40	*0.51	*0.68	
*0.41	*0.51	*0.68	
*0.41	*0.52	*0.70	

KEROGEN DESCRIPTION

Amorphous : 50 %
Exinite : 5 %
Vitrinite : 30 %
Inertinite : 15 %

Back Fluor : High
Bitumen : Small
Coke : None

DE LEE #1 - HITCHCOCK FIELD

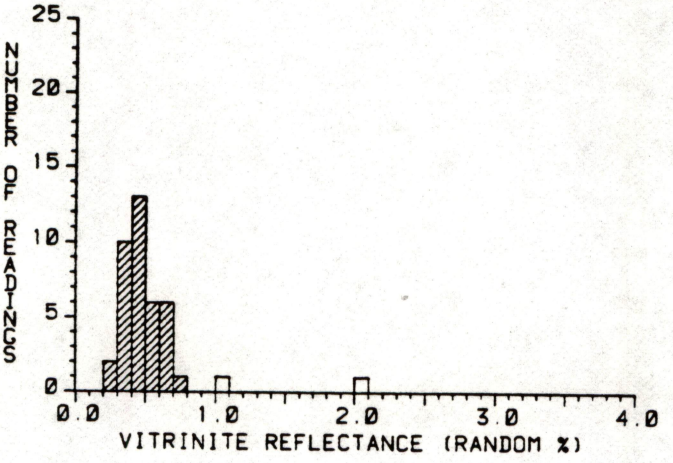

RRUS No. : 8
ID : CTGS.

DEPTH : 7392.0 Ft
: 2253.1 M

* = Ro MATURITY

VALUES : 38

MEAN : 0.46
STD DEV : 0.11
MEDIAN : 0.44
MODE : 0.45

HISTOGRAM:
Range: 0- 4%
Increment: 0.10%

ORDERED REFLECTANCE VALUES:

*0.29	*0.38	*0.44	*0.59
*0.29	*0.38	*0.44	*0.60
*0.32	*0.40	*0.46	*0.60
*0.33	*0.41	*0.46	*0.64
*0.34	*0.41	*0.49	*0.64
*0.35	*0.41	*0.51	*0.67
*0.36	*0.42	*0.52	*0.68
*0.36	*0.43	*0.56	*0.71
*0.37	*0.43	*0.56	1.03
*0.38	*0.44	*0.57	2.00

KEROGEN DESCRIPTION

Amorphous : 65 %
Exinite : 5 %
Vitrinite : 20 %
Inertinite : 10 %

Back Fluor : High
Bitumen : tr
Coke : tr

DE LEE #1 - HITCHCOCK FIELD

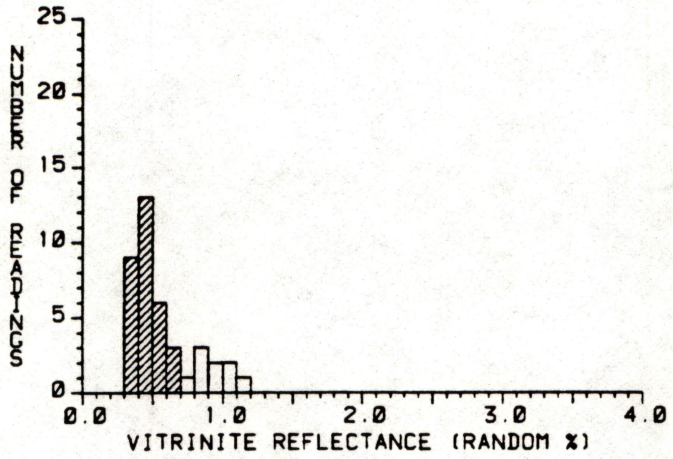

RRUS No. : 9
ID : CTGS.

DEPTH : 7534.0 Ft
: 2296.4 M

* = Ro MATURITY

VALUES : 31

MEAN : 0.46
STD DEV : 0.09
MEDIAN : 0.45
MODE : 0.45

HISTOGRAM:
Range: 0- 4%
Increment: 0.10%

ORDERED REFLECTANCE VALUES:

*0.33	*0.41	*0.48	*0.69
*0.34	*0.43	*0.49	0.78
*0.35	*0.43	*0.52	0.83
*0.36	*0.43	*0.54	0.86
*0.37	*0.44	*0.54	0.87
*0.37	*0.45	*0.55	0.90
*0.38	*0.45	*0.55	0.95
*0.39	*0.45	*0.55	1.05
*0.39	*0.45	*0.66	1.09
*0.41	*0.48	*0.66	1.13

KEROGEN DESCRIPTION

Amorphous : 35 %
Exinite : 10 %
Vitrinite : 40 %
Inertinite : 15 %

Back Fluor : High
Bitumen : tr
Coke : tr

DE LEE #1 - HITCHCOCK FIELD

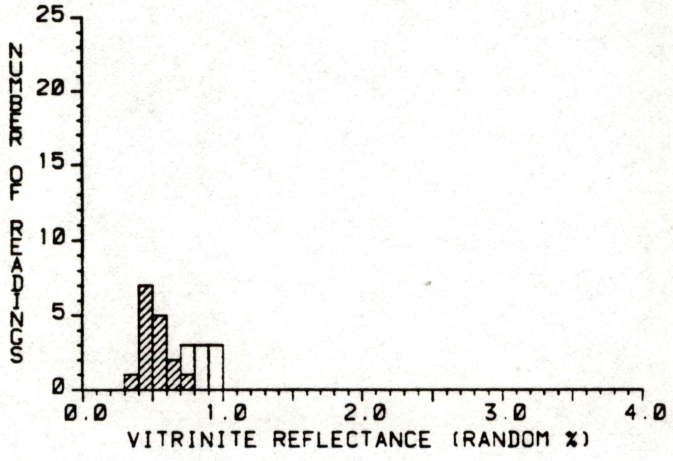

RRUS No. : 10
ID : CTGS.

DEPTH : 7677.0 Ft
: 2339.9 M

* = Ro MATURITY

VALUES : 16

MEAN : 0.51
STD DEV : 0.09
MEDIAN : 0.50
MODE : 0.45

HISTOGRAM:
Range: 0- 4%
Increment: 0.10%

ORDERED REFLECTANCE VALUES:

*0.39	*0.53	0.87
*0.41	*0.54	0.94
*0.41	*0.55	0.98
*0.44	*0.63	0.99
*0.47	*0.69	
*0.48	*0.71	
*0.48	0.76	
*0.49	0.79	
*0.50	0.81	
*0.50	0.84	

KEROGEN DESCRIPTION

Amorphous : 60 %
Exinite : 5 %
Vitrinite : 30 %
Inertinite : 5 %

Back Fluor : Med
Bitumen : tr
Coke : None

DE LEE #1 - HITCHCOCK FIELD

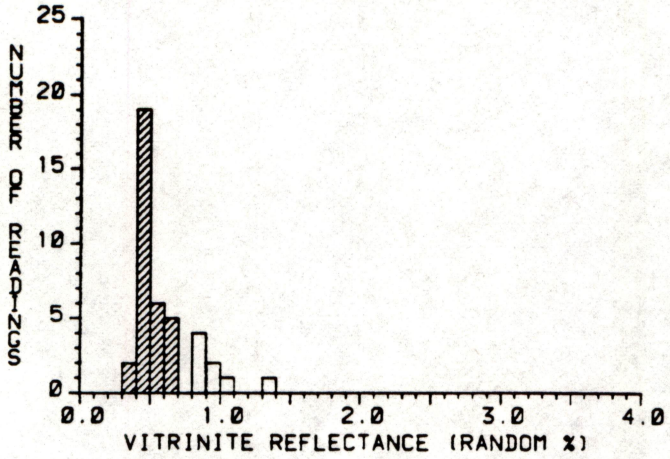

RRUS No. : 11
ID : CTGS.

DEPTH : 7858.0 Ft
: 2395.1 M

* = Ro MATURITY

VALUES : 32

MEAN : 0.49
STD DEV : 0.09
MEDIAN : 0.47
MODE : 0.45

HISTOGRAM:
Range: 0- 4%
Increment: 0.10%

ORDERED REFLECTANCE VALUES:

*0.30	*0.44	*0.49	*0.68
*0.37	*0.45	*0.51	*0.69
*0.40	*0.45	*0.52	0.80
*0.41	*0.46	*0.53	0.83
*0.41	*0.47	*0.55	0.86
*0.41	*0.47	*0.56	0.87
*0.42	*0.47	*0.58	0.90
*0.42	*0.48	*0.60	0.93
*0.44	*0.49	*0.63	1.02
*0.44	*0.49	*0.65	1.31

KEROGEN DESCRIPTION

Amorphous : 35 %
Exinite : 5 %
Vitrinite : 50 %
Inertinite : 10 %

Back Fluor : Med
Bitumen : tr
Coke : None

DE LEE #1 - HITCHCOCK FIELD

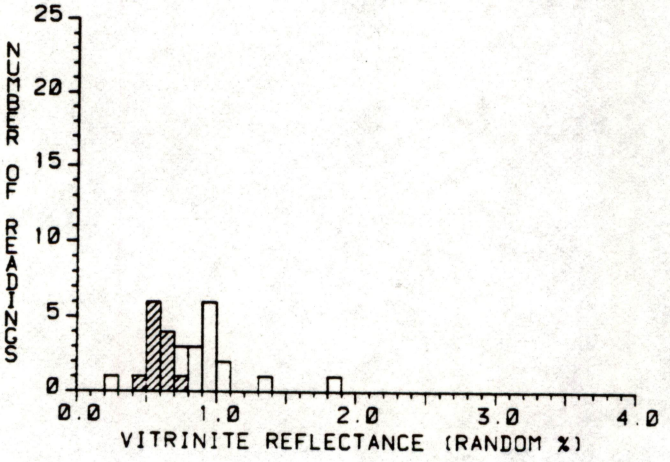

RRUS No. : 12
ID : CTGS.

DEPTH : 7990.0 Ft
: 2435.4 M

* = Ro MATURITY

VALUES : 12

MEAN : 0.58
STD DEV : 0.07
MEDIAN : 0.58
MODE : 0.55

HISTOGRAM:
Range: 0- 4%
Increment: 0.10%

ORDERED REFLECTANCE VALUES:

0.28	*0.63	0.95
*0.46	*0.67	0.95
*0.50	*0.70	0.97
*0.51	0.76	0.99
*0.52	0.77	1.00
*0.56	0.86	1.07
*0.58	0.87	1.38
*0.58	0.89	1.82
*0.60	0.90	
*0.62	0.92	

KEROGEN DESCRIPTION

Amorphous : 70 %
Exinite : 5 %
Vitrinite : 20 %
Inertinite : 2 %

Back Fluor : Med
Bitumen : tr
Coke : None

DE LEE #1 - HITCHCOCK FIELD

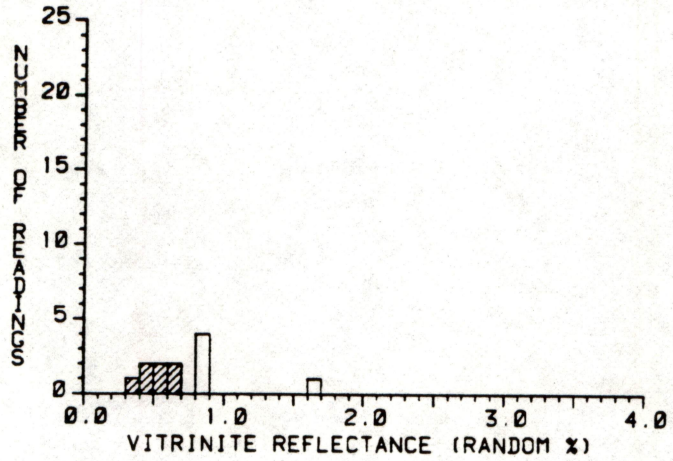

RRUS No. : 13
ID : CTGS.

DEPTH : 8126.0 Ft
: 2476.8 M

* = Ro MATURITY

VALUES : 7

MEAN : 0.52
STD DEV : 0.10
MEDIAN : 0.51
MODE : 0.65

HISTOGRAM:
Range: 0- 4%
Increment: 0.10%

ORDERED REFLECTANCE VALUES:

*0.38 0.85
*0.44 1.69
*0.49
*0.51
*0.52
*0.65
*0.66
0.81
0.82
0.83

KEROGEN DESCRIPTION

Amorphous : 80 %
Exinite : 0 %
Vitrinite : 10 %
Inertinite : 10 %

Back Fluor : Med
Bitumen : tr
Coke : None

DE LEE #1 - HITCHCOCK FIELD

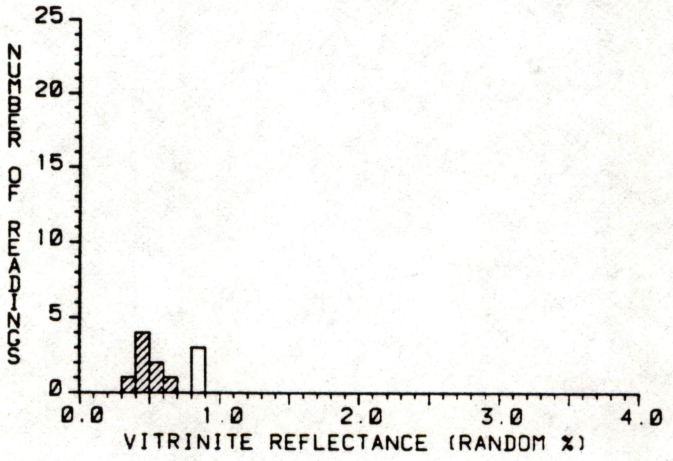

RRUS No. : 14
ID : CTGS.

DEPTH : 8304.0 Ft
: 2531.1 M

* = Ro MATURITY

VALUES : 8

MEAN : 0.47
STD DEV : 0.08
MEDIAN : 0.44
MODE : 0.45

HISTOGRAM:
Range: 0- 4%
Increment: 0.10%

ORDERED REFLECTANCE VALUES:

*0.37 0.89
*0.40
*0.42
*0.44
*0.44
*0.50
*0.59
*0.61
0.81
0.87

KEROGEN DESCRIPTION

Amorphous : 80 %
Exinite : 0 %
Vitrinite : 5 %
Inertinite : 15 %

Back Fluor : Med
Bitumen : tr
Coke : None

DE LEE #1 - HITCHCOCK FIELD

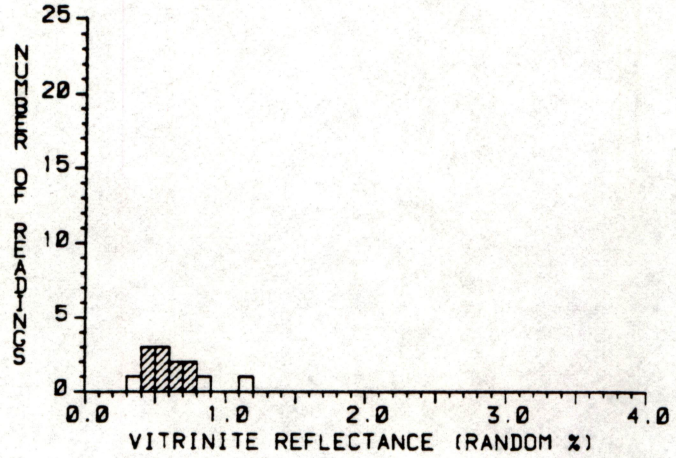

RRUS No. : 15
ID : CTGS.

DEPTH : 8429.0 Ft
: 2569.2 M

* = Ro MATURITY

VALUES : 10

MEAN : 0.57
STD DEV : 0.11
MEDIAN : 0.58
MODE : 0.55

HISTOGRAM:
Range: 0- 4%
Increment: 0.10%

ORDERED REFLECTANCE VALUES:

0.33	*0.72
*0.41	0.85
*0.43	1.12
*0.46	
*0.53	
*0.53	
*0.58	
*0.61	
*0.69	
*0.72	

KEROGEN DESCRIPTION

Amorphous	55 %
Exinite	15 %
Vitrinite	20 %
Inertinite	10 %
Back Fluor	Med
Bitumen	Small
Coke	None

DE LEE #1 - HITCHCOCK FIELD

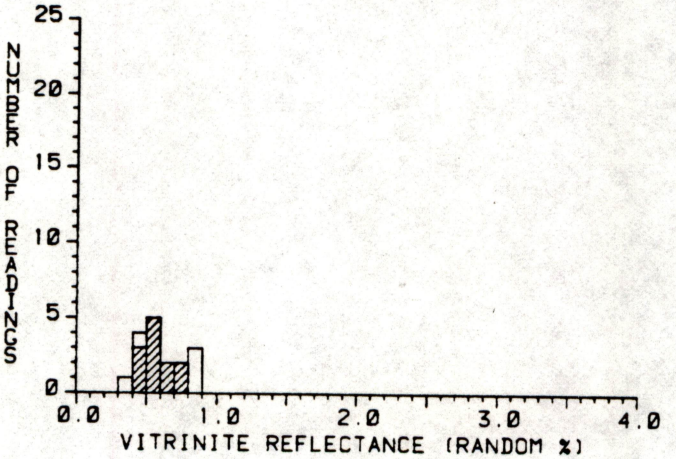

RRUS No. : 16
ID : CTGS.

DEPTH : 8602.0 Ft
: 2621.9 M

* = Ro MATURITY

VALUES : 12

MEAN : 0.57
STD DEV : 0.10
MEDIAN : 0.57
MODE : 0.55

HISTOGRAM:
Range: 0- 4%
Increment: 0.10%

ORDERED REFLECTANCE VALUES:

0.38	*0.60
0.40	*0.60
*0.44	*0.74
*0.46	*0.76
*0.46	0.83
*0.50	0.87
*0.55	0.88
*0.56	
*0.57	
*0.59	

KEROGEN DESCRIPTION

Amorphous	70 %
Exinite	50 %
Vitrinite	15 %
Inertinite	10 %
Back Fluor	Med
Bitumen	Small
Coke	None

DE LEE #1 - HITCHCOCK FIELD

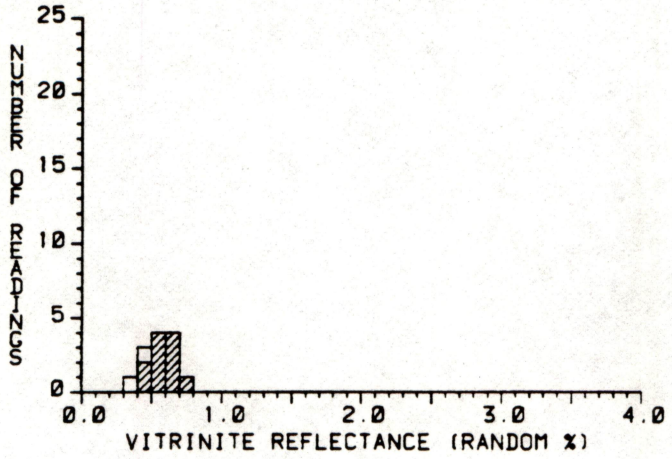

RRUS No. : 17
ID : CTGS.

DEPTH : 8759.0 Ft
: 2669.7 M

* = Ro MATURITY

VALUES : 11

MEAN : 0.58
STD DEV : 0.10
MEDIAN : 0.59
MODE : 0.65

HISTOGRAM:
Range: 0- 4%
Increment: 0.10%

ORDERED REFLECTANCE VALUES:

0.36	*0.64
0.40	*0.64
*0.42	*0.79
*0.43	
*0.50	
*0.54	
*0.56	
*0.59	
*0.61	
*0.63	

KEROGEN DESCRIPTION

Amorphous	75 %
Exinite	0 %
Vitrinite	15 %
Inertinite	10 %
Back Fluor	Low
Bitumen	tr
Coke	None

DE LEE #1 - HITCHCOCK FIELD

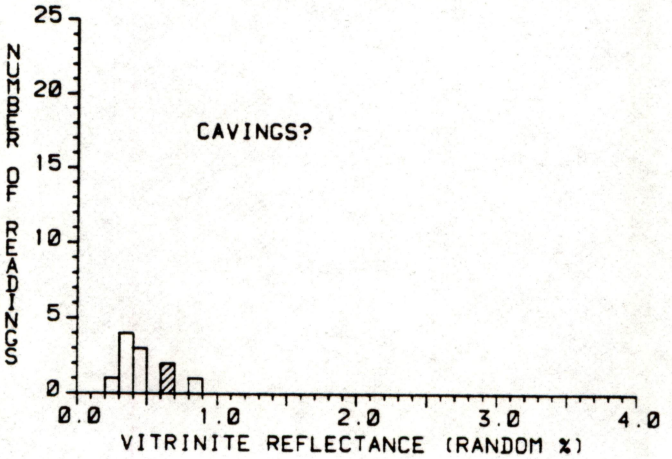

RRUS No. : 18
ID : CTGS.

DEPTH : 8913.0 Ft
: 2716.7 M

* = Ro MATURITY

VALUES : 2

MEAN : 0.65
STD DEV : 0.01
MEDIAN : 0.66
MODE : 0.65

HISTOGRAM:
Range: 0- 4%
Increment: 0.10%

ORDERED REFLECTANCE VALUES:

0.29	0.81
0.30	
0.30	
0.30	
0.36	
0.40	
0.42	
0.45	
*0.64	
*0.66	

KEROGEN DESCRIPTION

Amorphous	55 %
Exinite	5 %
Vitrinite	30 %
Inertinite	10 %
Back Fluor	Low
Bitumen	Small
Coke	None

DE LEE #1 - HITCHCOCK FIELD

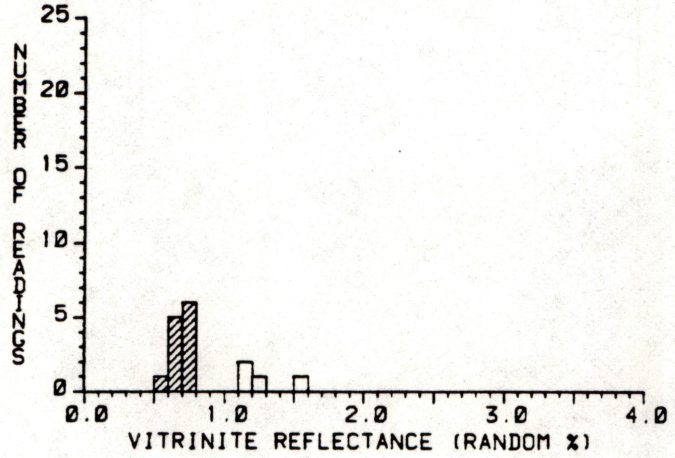

RRUS No. : 19
ID : CORE

DEPTH : 9070.0 Ft
: 2764.5 M

* = Ro MATURITY

VALUES : 12

MEAN : 0.68
STD DEV : 0.06
MEDIAN : 0.70
MODE : 0.75

HISTOGRAM:
Range: 0- 4%
Increment: 0.10%

ORDERED REFLECTANCE VALUES:

*0.58	*0.77
*0.61	*0.78
*0.64	1.12
*0.65	1.15
*0.65	1.23
*0.66	1.55
*0.70	
*0.70	
*0.72	
*0.72	

KEROGEN DESCRIPTION

Amorphous	60 %
Exinite	0 %
Vitrinite	30 %
Inertinite	10 %
Back Fluor	Low
Bitumen	tr
Coke	None

DE LEE #1 - HITCHCOCK FIELD

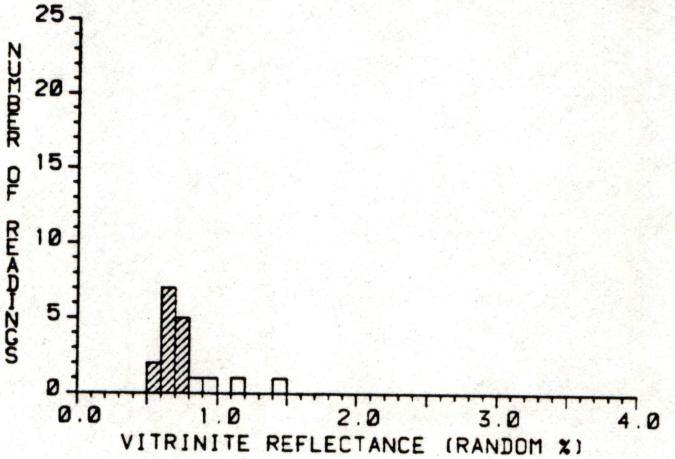

RRUS No. : 20
ID : CORE

DEPTH : 9083.0 Ft
: 2768.5 M

* = Ro MATURITY

VALUES : 14

MEAN : 0.66
STD DEV : 0.06
MEDIAN : 0.67
MODE : 0.65

HISTOGRAM:
Range: 0- 4%
Increment: 0.10%

ORDERED REFLECTANCE VALUES:

*0.55	*0.71
*0.59	*0.73
*0.61	*0.75
*0.62	*0.78
*0.62	0.83
*0.63	0.92
*0.65	1.14
*0.67	1.43
*0.68	
*0.70	

KEROGEN DESCRIPTION

Amorphous	45 %
Exinite	5 %
Vitrinite	40 %
Inertinite	10 %
Back Fluor	Low
Bitumen	tr
Coke	None

DE LEE #1 - HITCHCOCK FIELD

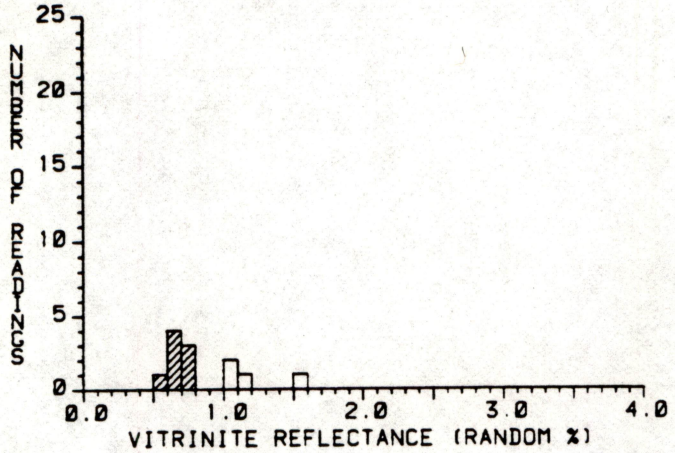

RRUS No. : 21
ID : CORE

DEPTH : 9092.0 Ft
: 2771.2 M

* = Ro MATURITY

VALUES : 8

MEAN : 0.67
STD DEV : 0.06
MEDIAN : 0.68
MODE : 0.65

HISTOGRAM:
Range: 0- 4%
Increment: 0.10%

ORDERED REFLECTANCE VALUES:

*0.53	1.16
*0.65	1.54
*0.65	
*0.67	
*0.68	
*0.71	
*0.71	
*0.76	
1.00	
1.04	

KEROGEN DESCRIPTION

Amorphous	30 %
Exinite	0 %
Vitrinite	65 %
Inertinite	5 %
Back Fluor	None
Bitumen	None
Coke	None

DE LEE #1 - HITCHCOCK FIELD

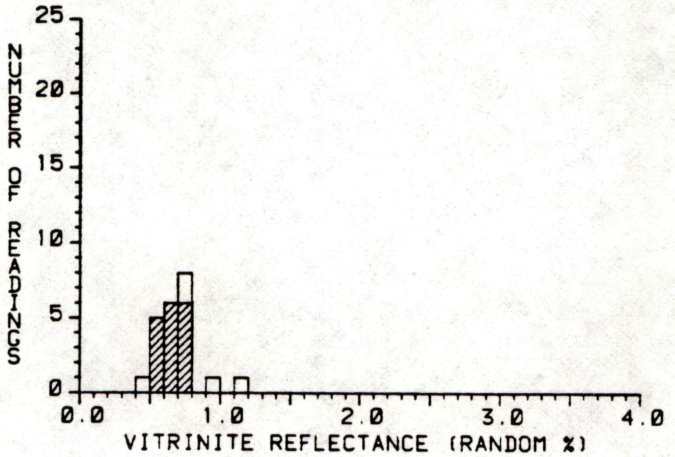

RRUS No. : 22
ID : CORE

DEPTH : 9099.0 Ft
: 2773.4 M

* = Ro MATURITY

VALUES : 17

MEAN : 0.64
STD DEV : 0.08
MEDIAN : 0.65
MODE : 0.75

HISTOGRAM:
Range: 0- 4%
Increment: 0.10%

ORDERED REFLECTANCE VALUES:

0.43	*0.65	0.93
*0.50	*0.69	1.13
*0.51	*0.70	
*0.56	*0.71	
*0.57	*0.71	
*0.58	*0.72	
*0.60	*0.74	
*0.61	*0.76	
*0.63	0.79	
*0.65	0.79	

KEROGEN DESCRIPTION

Amorphous	25 %
Exinite	0 %
Vitrinite	65 %
Inertinite	10 %
Back Fluor	Low
Bitumen	tr
Coke	None

DE LEE #1 - HITCHCOCK FIELD

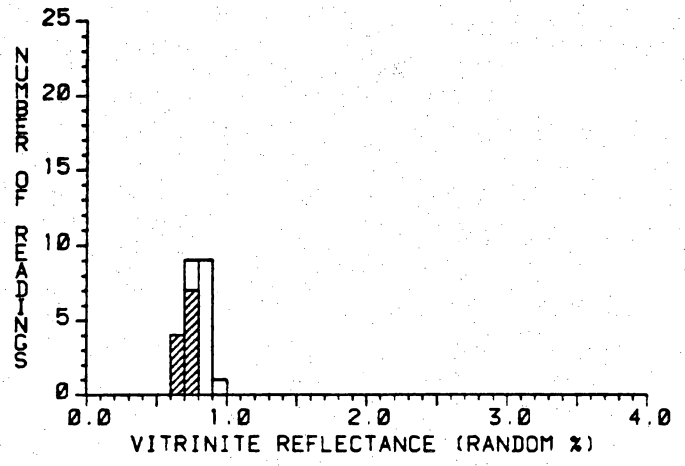

RRUS No. : 23
ID : CORE

DEPTH : 9100.0 Ft
: 2773.7 M

* = Ro MATURITY

VALUES : 11

MEAN : 0.70
STD DEV : 0.04
MEDIAN : 0.71
MODE : 0.75

HISTOGRAM:
Range: 0- 4%
Increment: 0.10%

ORDERED REFLECTANCE VALUES:

*0.63	*0.74	0.88
*0.64	0.78	0.88
*0.66	0.79	0.92
*0.67	0.80	
*0.70	0.81	
*0.71	0.81	
*0.72	0.83	
*0.73	0.84	
*0.74	0.86	
*0.74	0.87	

KEROGEN DESCRIPTION

Amorphous	20 %
Exinite	10 %
Vitrinite	60 %
Inertinite	10 %
Back Fluor	Med
Bitumen	tr
Coke	None

DE LEE #1 - HITCHCOCK FIELD

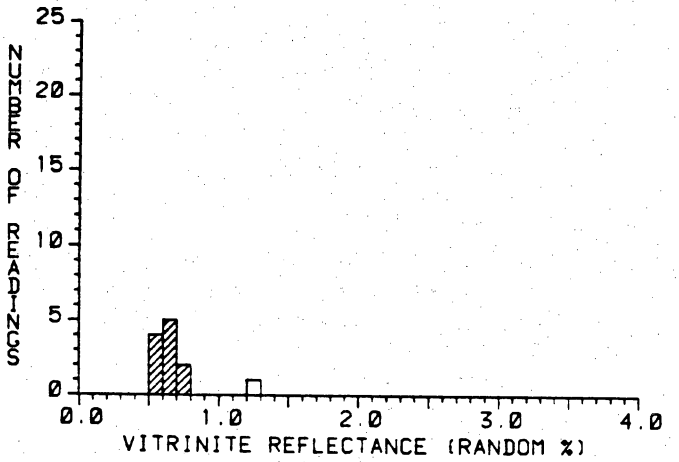

RRUS No. : 24
ID : CORE

DEPTH : 9100.5 Ft
: 2773.8 M

* = Ro MATURITY

VALUES : 11

MEAN : 0.64
STD DEV : 0.07
MEDIAN : 0.67
MODE : 0.65

HISTOGRAM:
Range: 0- 4%
Increment: 0.10%

ORDERED REFLECTANCE VALUES:

*0.50	*0.75
*0.56	1.29
*0.57	
*0.58	
*0.63	
*0.67	
*0.68	
*0.69	
*0.69	
*0.71	

KEROGEN DESCRIPTION

Amorphous	55 %
Exinite	10 %
Vitrinite	30 %
Inertinite	5 %
Back Fluor	Low
Bitumen	None
Coke	None

DE LEE #1 - HITCHCOCK FIELD

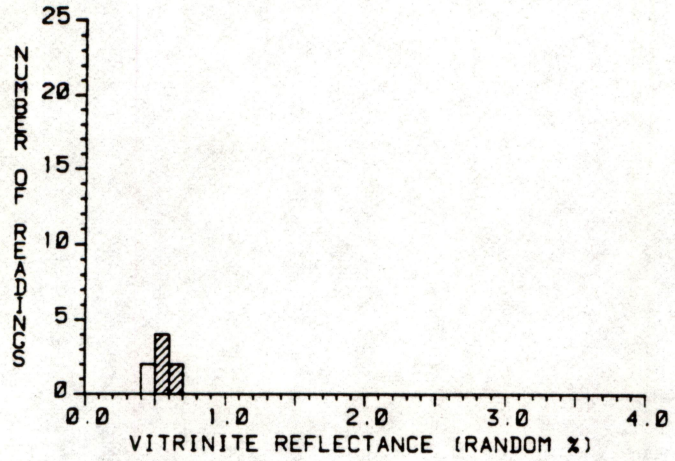

RRUS No. : 25
ID : CORE

DEPTH : 9100.7 Ft
: 2773.9 M

* = Ro MATURITY

VALUES : 6

MEAN : 0.59
STD DEV : 0.05
MEDIAN : 0.59
MODE : 0.55

HISTOGRAM:
Range: 0- 4%
Increment: 0.10%

ORDERED REFLECTANCE VALUES:

0.47
0.47
*0.54
*0.55
*0.56
*0.59
*0.63
*0.68

KEROGEN DESCRIPTION

Amorphous	:	60 %
Exinite	:	5 %
Vitrinite	:	15 %
Inertinite	:	20 %
Back Fluor	:	None
Bitumen	:	None
Coke	:	None

DE LEE #1 - HITCHCOCK FIELD

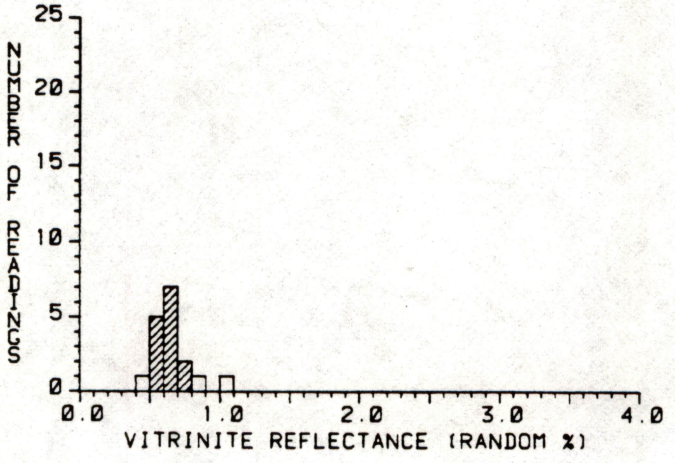

RRUS No. : 26
ID : CORE

DEPTH : 9100.8 Ft
: 2773.9 M

* = Ro MATURITY

VALUES : 14

MEAN : 0.64
STD DEV : 0.06
MEDIAN : 0.63
MODE : 0.65

HISTOGRAM:
Range: 0- 4%
Increment: 0.10%

ORDERED REFLECTANCE VALUES:

0.48	*0.66
*0.56	*0.68
*0.56	*0.69
*0.57	*0.72
*0.58	*0.77
*0.59	0.87
*0.62	1.00
*0.63	
*0.63	
*0.65	

KEROGEN DESCRIPTION

Amorphous	:	45 %
Exinite	:	15 %
Vitrinite	:	30 %
Inertinite	:	10 %
Back Fluor	:	Low
Bitumen	:	Small
Coke	:	None

DE LEE #1 - HITCHCOCK FIELD

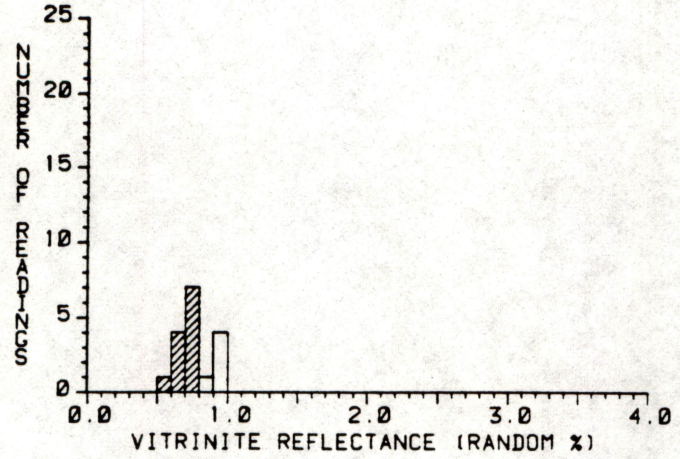

RRUS No. : 27
ID : CORE

DEPTH : 9101.0 Ft
: 2774.0 M

* = Ro MATURITY

VALUES : 12

MEAN : 0.70
STD DEV : 0.06
MEDIAN : 0.72
MODE : 0.75

HISTOGRAM:
Range: 0- 4%
Increment: 0.10%

ORDERED REFLECTANCE VALUES:

*0.58	*0.77
*0.61	*0.78
*0.65	0.83
*0.66	0.90
*0.67	0.93
*0.70	0.94
*0.72	0.99
*0.74	
*0.75	
*0.77	

KEROGEN DESCRIPTION

Amorphous	75 %
Exinite	0 %
Vitrinite	15 %
Inertinite	10 %
Back Fluor	Low
Bitumen	tr
Coke	None

DE LEE #1 - HITCHCOCK FIELD

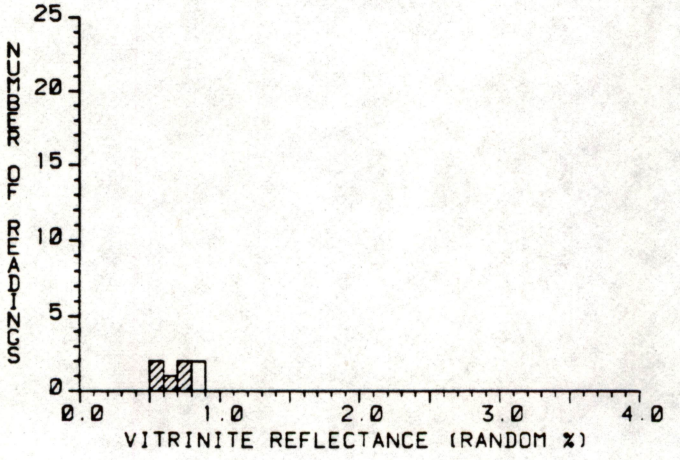

RRUS No. : 28
ID : CORE

DEPTH : 9103.3 Ft
: 2774.7 M

* = Ro MATURITY

VALUES : 5

MEAN : 0.66
STD DEV : 0.08
MEDIAN : 0.66
MODE : 0.75

HISTOGRAM:
Range: 0- 4%
Increment: 0.10%

ORDERED REFLECTANCE VALUES:

*0.57	
*0.58	
*0.66	
*0.74	
*0.76	
0.80	
0.84	

KEROGEN DESCRIPTION

Amorphous	85 %
Exinite	0 %
Vitrinite	10 %
Inertinite	5 %
Back Fluor	Med
Bitumen	Small
Coke	None

DE LEE #1 - HITCHCOCK FIELD

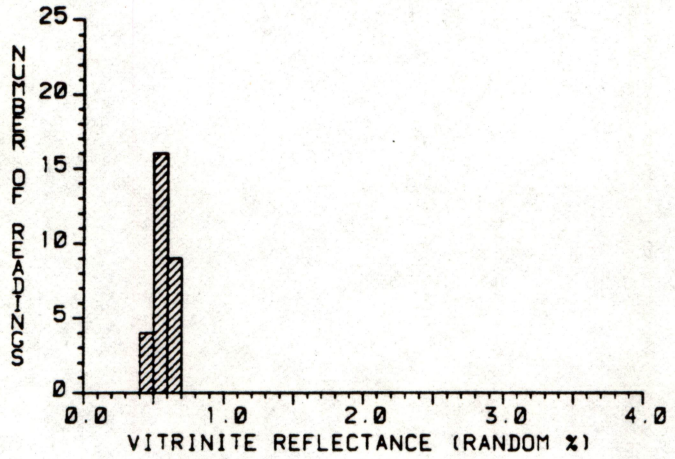

RRUS No. : 29
ID : CORE

DEPTH : 9104.5 Ft
: 2775.1 M

* = Ro MATURITY

VALUES : 29

MEAN : 0.56
STD DEV : 0.05
MEDIAN : 0.55
MODE : 0.55

HISTOGRAM:
Range: 0- 4%
Increment: 0.10%

ORDERED REFLECTANCE VALUES:

*0.45	*0.53	*0.60
*0.46	*0.54	*0.60
*0.49	*0.55	*0.61
*0.49	*0.55	*0.61
*0.51	*0.55	*0.61
*0.51	*0.56	*0.62
*0.52	*0.56	*0.63
*0.53	*0.58	*0.64
*0.53	*0.58	*0.65
*0.53	*0.59	

KEROGEN DESCRIPTION

Amorphous : 40 %
Exinite : 5 %
Vitrinite : 50 %
Inertinite : 5 %

Back Fluor : Low
Bitumen : None
Coke : None

DE LEE #1 - HICHCOCK FIELD

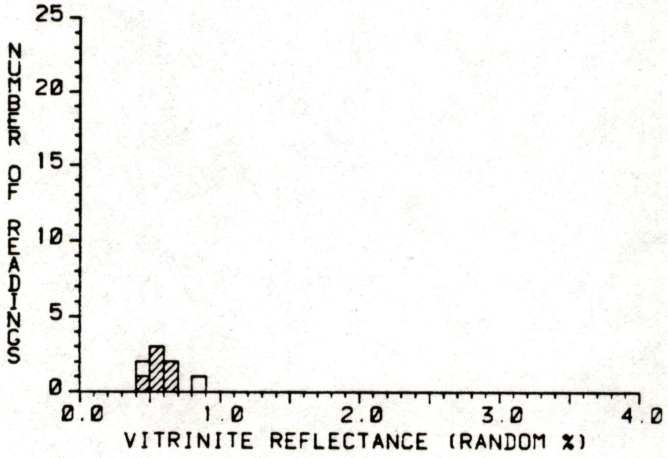

RRUS No. : 30
ID : CORE

DEPTH : 9125.0 Ft
: 2781.3 M

* = Ro MATURITY

VALUES : 6

MEAN : 0.58
STD DEV : 0.06
MEDIAN : 0.59
MODE : 0.55

HISTOGRAM:
Range: 0- 4%
Increment: 0.10%

ORDERED REFLECTANCE VALUES:

0.44
*0.49
*0.56
*0.58
*0.59
*0.62
*0.67
0.80

KEROGEN DESCRIPTION

Amorphous : 55 %
Exinite : tr %
Vitrinite : 35 %
Inertinite : 10 %

Back Fluor : Low
Bitumen : Small
Coke : None

DE LEE #1 - HITCHCOCK FIELD

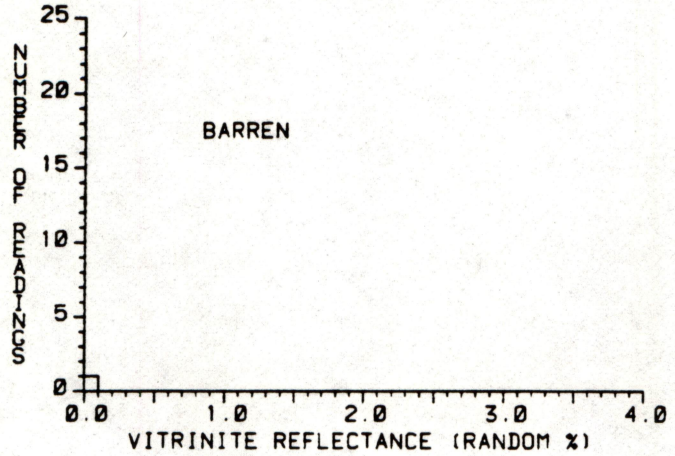

RRUS No. : 31
ID : CORE

DEPTH : 9141.0 Ft
: 2786.2 M

MEAN : N.D.

HISTOGRAM:
Range: 0- 4%
Increment: 0.10%

ORDERED REFLECTANCE VALUES:

0.00

KEROGEN DESCRIPTION

Amorphous	:	95 %
Exinite	:	0 %
Vitrinite	:	5 %
Inertinite	:	tr %
Back Fluor	:	Med
Bitumen	:	tr
Coke	:	None

DE LEE #1 - HITCHCOCK FIELD

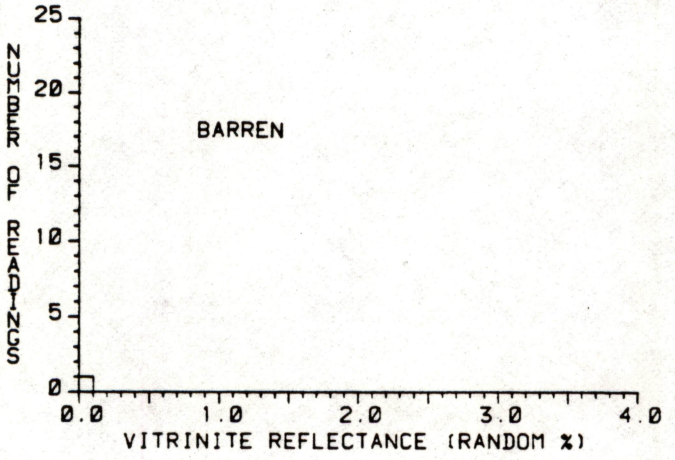

RRUS No. : 32
ID : CORE

DEPTH : 9149.0 Ft
: 2788.6 M

MEAN : N.D.

HISTOGRAM:
Range: 0- 4%
Increment: 0.10%

ORDERED REFLECTANCE VALUES:

0.00

KEROGEN DESCRIPTION

Amorphous	:	90 %
Exinite	:	0 %
Vitrinite	:	5 %
Inertinite	:	5 %
Back Fluor	:	Low
Bitumen	:	Small
Coke	:	None

DE LEE #1 - HITCHCOCK FIELD

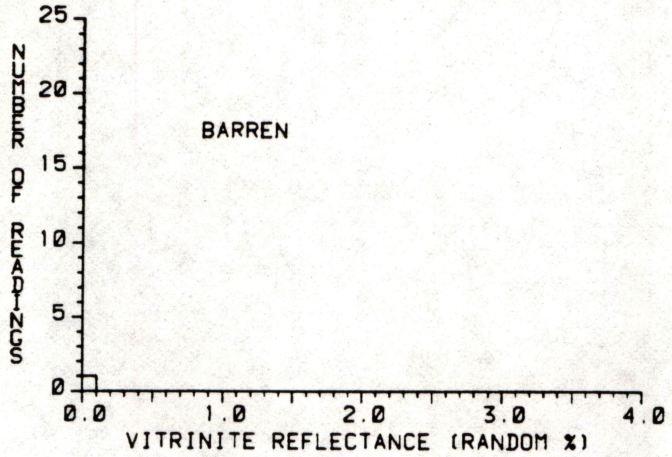

RRUS No. : 33
ID : CORE

DEPTH : 9167.5 Ft
: 2794.3 M

MEAN : N.D.

HISTOGRAM:
Range: 0- 4%
Increment: 0.10%

ORDERED REFLECTANCE VALUES:

0.00

KEROGEN DESCRIPTION

Amorphous	:	90 %
Exinite	:	0 %
Vitrinite	:	5 %
Inertinite	:	5 %
Back Fluor	:	Low
Bitumen	:	tr
Coke	:	None

DE LEE #1 - HITCHCOCK FIELD

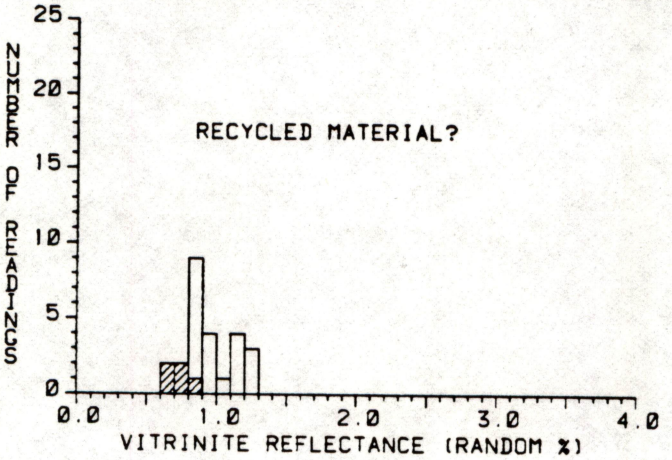

RRUS No. : 34
ID : CORE

DEPTH : 9179.9 Ft
: 2798.0 M

* = Ro MATURITY

VALUES : 5

MEAN	:	0.73
STD DEV	:	0.07
MEDIAN	:	0.79
MODE	:	0.75

HISTOGRAM:
Range: 0- 4%
Increment: 0.10%

ORDERED REFLECTANCE VALUES:

*0.62	0.84	1.14
*0.67	0.87	1.16
*0.79	0.89	1.21
*0.79	0.91	1.23
*0.80	0.93	1.26
0.82	0.93	
0.82	0.99	
0.82	1.06	
0.82	1.10	
0.82	1.12	

KEROGEN DESCRIPTION

Amorphous	:	45 %
Exinite	:	0 %
Vitrinite	:	35 %
Inertinite	:	20 %
Back Fluor	:	Low
Bitumen	:	tr
Coke	:	None

DE LEE #1 - HITCHCOCK FIELD

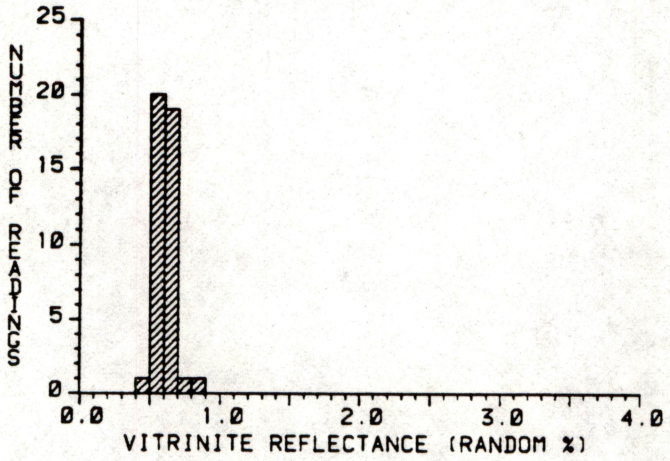

RRUS No. : 35
ID : CORE

DEPTH : 9194.3 Ft
: 2802.4 M

* = Ro MATURITY

VALUES : 42

MEAN : 0.60
STD DEV : 0.06
MEDIAN : 0.60
MODE : 0.55

HISTOGRAM:
Range: 0- 4%
Increment: 0.10%

ORDERED REFLECTANCE VALUES:

*0.49	*0.56	*0.59	*0.64	*0.70
*0.50	*0.56	*0.60	*0.64	*0.83
*0.52	*0.57	*0.60	*0.64	
*0.54	*0.57	*0.61	*0.64	
*0.54	*0.57	*0.61	*0.65	
*0.54	*0.57	*0.61	*0.65	
*0.55	*0.58	*0.62	*0.66	
*0.55	*0.59	*0.63	*0.67	
*0.55	*0.59	*0.63	*0.67	
*0.56	*0.59	*0.63	*0.68	

KEROGEN DESCRIPTION

Amorphous : 35 %
Exinite : 5 %
Vitrinite : 50 %
Inertinite : 10 %

Back Fluor : Low
Bitumen : Small
Coke : None

DE LEE #1 - HITCHCOCK FIELD

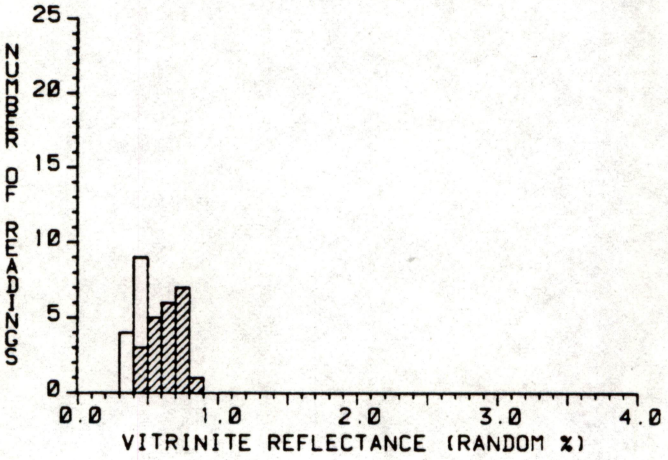

RRUS No. : 36
ID : CORE

DEPTH : 9262.0 Ft
: 2823.1 M

* = Ro MATURITY

VALUES : 22

MEAN : 0.63
STD DEV : 0.10
MEDIAN : 0.63
MODE : 0.75

HISTOGRAM:
Range: 0- 4%
Increment: 0.10%

ORDERED REFLECTANCE VALUES:

0.31	*0.46	*0.63	*0.76
0.33	*0.48	*0.63	*0.81
0.37	*0.49	*0.67	
0.38	*0.50	*0.69	
0.40	*0.50	*0.70	
0.41	*0.54	*0.70	
0.42	*0.59	*0.70	
0.43	*0.59	*0.71	
0.43	*0.61	*0.71	
0.44	*0.61	*0.72	

KEROGEN DESCRIPTION

Amorphous : 45 %
Exinite : 10 %
Vitrinite : 35 %
Inertinite : 10 %

Back Fluor : Low
Bitumen : tr
Coke : None

DE LEE #1 - HITCHCOCK FIELD

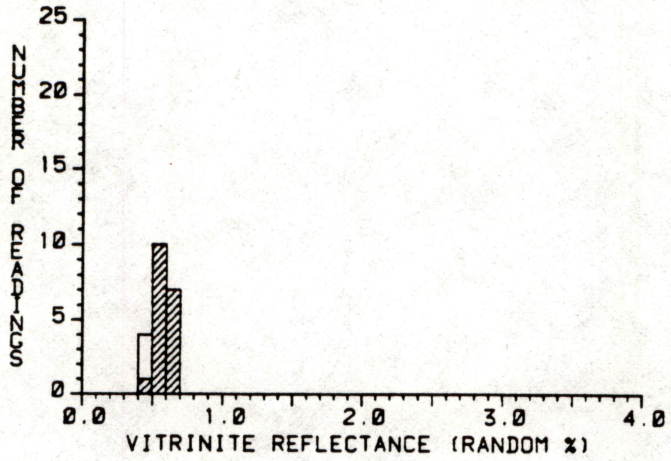

RRUS No. : 37
ID : CTGS.

DEPTH : 9302.0 Ft
: 2835.2 M

* = Ro MATURITY

VALUES : 18

MEAN : 0.58
STD DEV : 0.07
MEDIAN : 0.59
MODE : 0.55

HISTOGRAM:
Range: 0- 4%
Increment: 0.10%

ORDERED REFLECTANCE VALUES:

0.40	*0.54	*0.69
0.45	*0.56	
0.47	*0.59	
*0.49	*0.59	
*0.50	*0.63	
*0.51	*0.63	
*0.51	*0.63	
*0.51	*0.65	
*0.52	*0.67	
*0.53	*0.67	

KEROGEN DESCRIPTION

Amorphous	40 %
Exinite	15 %
Vitrinite	35 %
Inertinite	10 %
Back Fluor	Med
Bitumen	tr
Coke	None

DE LEE #1 - HITCHCOCK FIELD

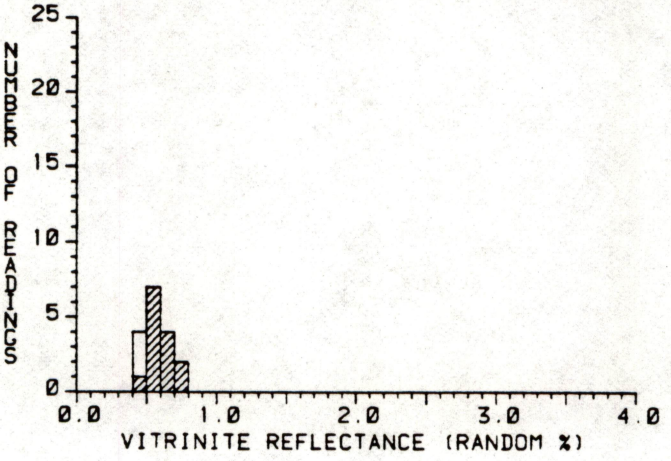

RRUS No. : 38
ID : CTGS.

DEPTH : 9340.0 Ft
: 2846.8 M

* = Ro MATURITY

VALUES : 14

MEAN : 0.60
STD DEV : 0.09
MEDIAN : 0.58
MODE : 0.55

HISTOGRAM:
Range: 0- 4%
Increment: 0.10%

ORDERED REFLECTANCE VALUES:

0.45	*0.58
0.45	*0.61
0.47	*0.63
*0.48	*0.67
*0.50	*0.68
*0.53	*0.76
*0.53	*0.78
*0.56	
*0.56	
*0.58	

KEROGEN DESCRIPTION

Amorphous	30 %
Exinite	5 %
Vitrinite	50 %
Inertinite	15 %
Back Fluor	Low
Bitumen	tr
Coke	None

DE LEE #1 - HITCHCOCK FIELD

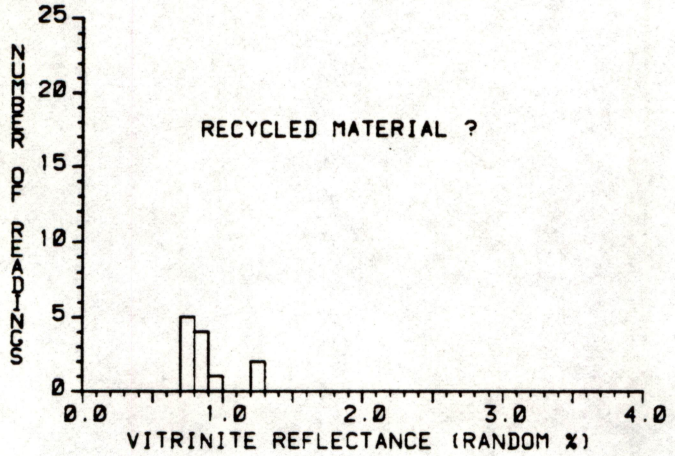

RRUS No. : 39
ID : CTGS.

DEPTH : 9367.0 Ft
: 2855.1 M

MEAN : N.D.

HISTOGRAM:
Range: 0- 4%
Increment: 0.10%

ORDERED REFLECTANCE VALUES:

0.70	1.23
0.72	1.25
0.73	
0.74	
0.78	
0.81	
0.81	
0.82	
0.86	
0.95	

KEROGEN DESCRIPTION

Amorphous	40 %
Exinite	5 %
Vitrinite	40 %
Inertinite	15 %
Back Fluor	Med
Bitumen	None
Coke	None

DE LEE #1 HITCHCOCK FIELD

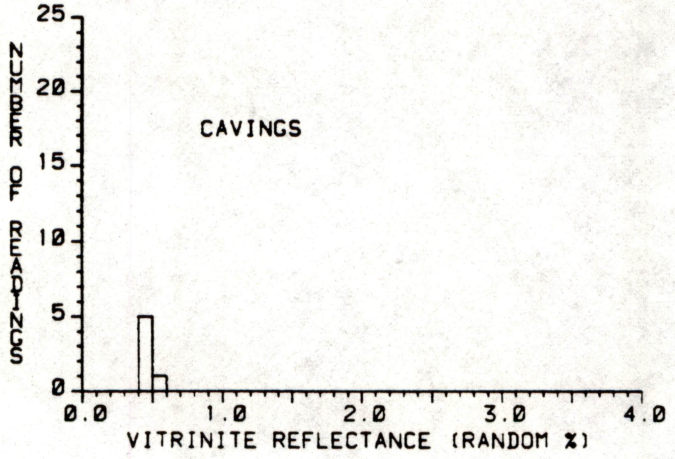

RRUS No. : 40
ID : CTGS.

DEPTH : 9392.0 Ft
: 2862.7 M

MEAN : N.D.

HISTOGRAM:
Range: 0- 4%
Increment: 0.10%

ORDERED REFLECTANCE VALUES:

0.42
0.43
0.47
0.48
0.49
0.50

KEROGEN DESCRIPTION

Amorphous	45 %
Exinite	5 %
Vitrinite	40 %
Inertinite	10 %
Back Fluor	None
Bitumen	tr
Coke	None

Detailed Compositional Data for Crude Oil

Sample No. 3013-041

GROSS OIL COMPOSITION (%)

Less than C_{15+} Fraction	58.3
C_{15+} Fraction	41.7

C_{15+} OIL COMPOSITION (%)

Asphaltene(ASPH)	1.0
Paraffin-Naphthene(P-N)	81.3
Aromatic HC(AROM)	16.7
Eluted NSO	0.5
Non-eluted NSO	0.5

DETAILED C_4-C_7 COMPOSITION (NORM.%)

Isobutane
n-Butane
Isopentane
n-Pentane
2,2-Dimethylbutane
Cyclopentane
2,3-Dimethylbutane
2-Methylpentane
3-Methylpentane
n-Hexane
Methylcyclopentane
2,2-Dimethylpentane
Benzene
2,4-Dimethylpentane
2,2,3-Trimethylbutane
Cyclohexane
3,3-Dimethylpentane
1,1-Dimethylcyclopentane
2-Methylhexane
2,3-Dimethylpentane
1,cis-3-Dimethylcyclopentane
3-Methylhexane
1,trans-3-Dimethylcyclopentane
1,trans-2-Dimethylcyclopentane
3-Ethylpentane
n-Heptane
1,cis-2-Dimethylcyclopentane
Methylcyclohexane
Toluene

COMPOSITION OF C_{15+} SATURATE HYDROCARBONS

% n-Alkanes	36.3
% Isoalkanes	5.6
% C_{19} & C_{20} Isoprenoids	
% Naphthenes	58.1
Sat/Arom	4.86
Asph/NSO	1.00
CPI Index A	1.06
CPI Index B	1.08
ip-C_{19}/ip-C_{20}	2.69

NORMALIZED PARAFFIN DISTRIBUTION (%)

nC_{15}
nC_{16}
nC_{17}
ip-C_{19}
nC_{18}
ip-C_{20}
nC_{19}
nC_{20}
nC_{21}
nC_{22}
nC_{23}
nC_{24}
nC_{25}
nC_{26}
nC_{27}
nC_{28}
nC_{29}
nC_{30}
nC_{31}
nC_{32}
nC_{33}
nC_{34}
nC_{35}

MOLECULAR RATIOS

2-methylpentane/3-methylpentane
isopentane/n-pentane
cyclohexane/methylcyclopentane
methycyclopentane/methylcyclohexane

DETAILED C4-C7 HYDROCARBON ANALYSES

(NORMALIZED PERCENT)

GEOCHEM SAMPLE NUMBER	3013-041
CLIENT I.D. NO.	N.E. Hitchcock Field
ISOBUTANE	4.0
N-BUTANE	5.6
ISOPENTANE	8.1
N-PENTANE	7.6
2,2-DIMETHYLBUTANE	1.0
CYCLOPENTANE	0.7
2,3-DIMETHYLBUTANE	1.6
2-METHYLPENTANE	6.1
3-METHYLPENTANE	3.7
N-HEXANE	8.2
METHYCYCLOPENTANE	3.7
2,2-DIMETHYLPENTANE	0.6
BENZENE	1.3
2,4-DIMETHYLPENTANE	0.9
2,2,3-TRIMETHYLBUTANE	0.3
CYCLOHEXANE	6.4
3,3-DIMETHYLPENTANE	0.4
1,1-DIMETHYLCYCLOPENTANE	0.7
2-METHYLHEXANE	4.6
2,3-DIMETHYLPENTANE	0.0
1,CIS-3-DIMETHYLCYCLOPENTANE	0.7
3-METHYLHEXANE	3.7
1 TRANS-3-DIMETHYLCYCLOPENTANE	0.3
1 TRANS-2-DIMETHYLCYCLOPENTANE	1.3
3-ETHYLPENTANE	0.3
2,2,4-TRIMETHYLPENTANE	0.0
N-HEPTANE	6.5
1,CIS-2-DIMETHYLCYCLOPENTANE	0.2
METHYCYCLOHEXANE	10.0
1,1,3-TRIMETHYLCYCLOPENTANE *	0.4
2,2-DIMETHYLHEXANE	0.3
ETHYLCYCLOPENTANE	0.4
TOLUENE	10.3
C4-C7 HYDROCARBON CONTENT/PPM**	1.7

MOLECULAR RATIOS

2-METHYLPENTANE/3-METHYLPENTANE	1.66
ISOPENTANE/N-PENTANE	1.07
CYCLOHEXANE/METHYLCYCLOPENTANE	1.70
METHYLCYCLOPENT/METHYLCYCLOHEX	0.38

* C8 COMPOUNDS

** PPM VALUES ARE EXPRESSED AS VOLUMES OF GAS PER MILLION VOLUMES OF CUTTINGS

CRUDE OIL ANALYSIS RESULTS

GeoChem Sample No.: 3013-041
Client Identification No.: N.E. Hitchcock Field

GROSS COMPOSITION

Less than C_{15+}	58.3%
C_{15+}	41.7%

C_{15+} COMPOSITION

Asphaltene (ASPH)	1.0%
Paraffin-Naphthene Hydrocarbons (P-N)	81.3%
Aromatic Hydrocarbons (AROM)	16.7%
Eluted NSO Compounds (NSO)	0.5%
Noneluted NSO Compounds (NSO)	0.5%

RATIOS

$$\frac{P\text{-}N}{AROM} = 4.86$$

$$\frac{ASPH}{NSO} = 1.00$$

Saturate Hydrocarbon Analyses

Summary of Paraffin-Naphthene Distribution

GeoChem Sample Number	Client Identification Number	% Paraffin	% Isoprenoid	% Naphthene	C-P Index A	C-P Index B	ip19/ip20
3013-041	N. E. Hitchcock Field	36.3	5.6	58.1	1.06	1.08	2.69

Saturate Hydrocarbon Analyses

Normalized Paraffin Distribution

GeoChem Sample Number	Client Identification Number	% nC15	% nC16	% nC17	% ip19	% nC18	% ip20	% nC19	% nC20	% nC21	% nC22	% nC23	% nC24	% nC25	% nC26	% nC27	% nC28	% nC29	% nC30	% nC31	% nC32	% nC33	% nC34	% nC35
3013-041	N.E. Hitchcock Field	14.1	12.5	9.4	9.8	8.2	3.6	7.2	6.3	5.5	4.4	4.0	3.4	2.9	2.3	1.9	1.3	1.1	0.7	0.5	0.4	0.2	0.2	0.1

C_{15+} Paraffin-Naphthene (P-N) Hydrocarbon

GeoChem Sample No. 3013-041

Client I.D. No. N.E. Hitchcock Field

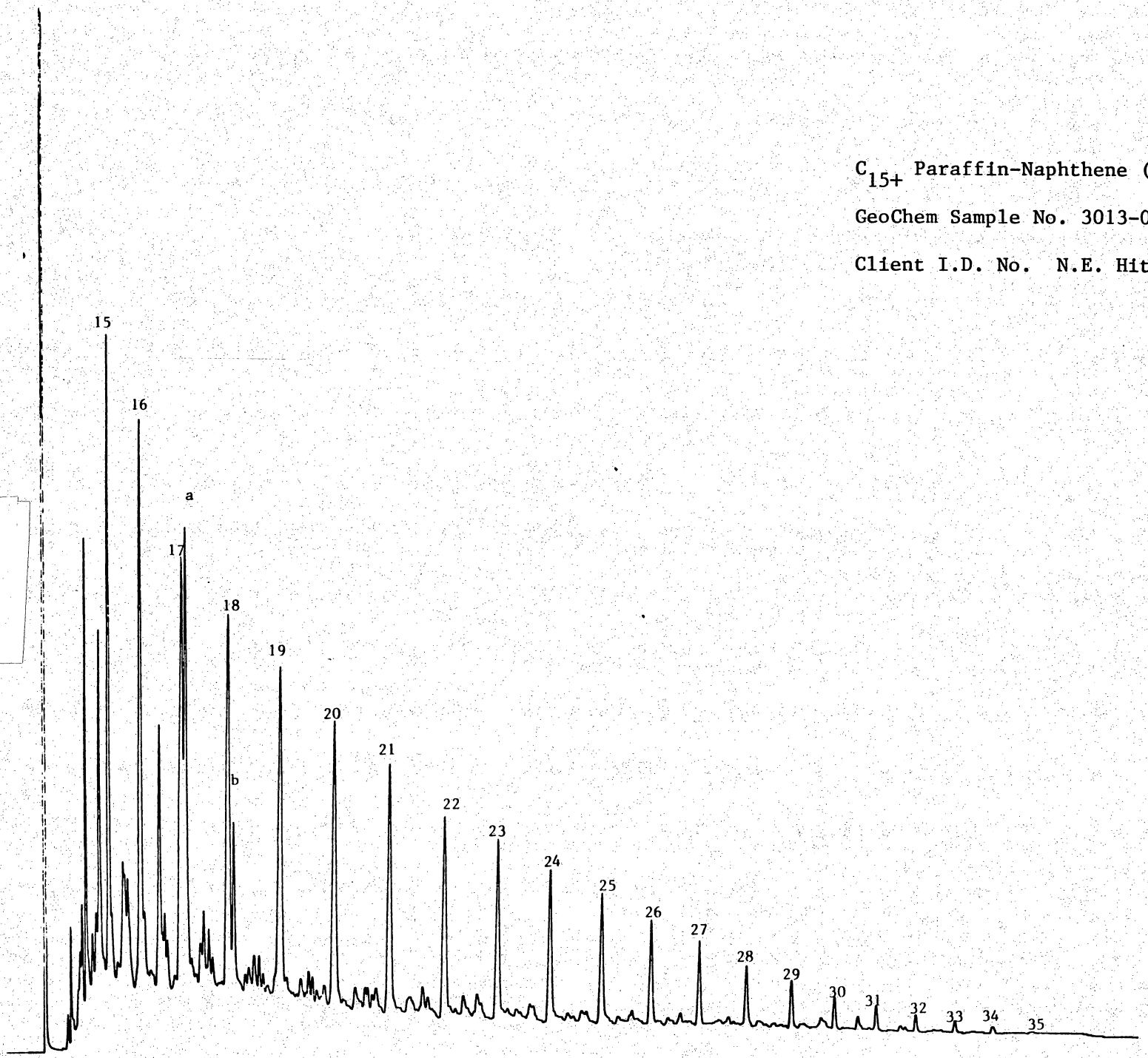

List of Figures

Figure 13. Burial history diagram of the Hitchcock N.E. field.

Figure 14. Maturation profile of the Delee No. 1 well based on vitrinite reflectance data compared to a maturation profile for the Hitchcock N.E. field using Lopatin's method (Waples, 1980).

Figure 15. Temperature profiles in a geopressured zone, modified from Lewis and Rose (1970).

Figure 16. Natural logarithm of the naphthene fraction in shale extracts versus the natural logarithm of the time-temperature integral for the Pleasant Bayou No. 1 geothermal test well. For comparison the natural logarithm of the naphthene fraction of oil from the Prets No. 1 well is shown. Age ranges of the naphthene fractions are from Young and others (1977).

Figure 17. KFC diagram showing the elemental compositions of Anahuac and Frio shales compared to pure clay end members (Deer and others, 1969). The estimated illite and silica concentration in the clays is also shown.

Figure 18. Estimated concentrations of illite, silica, and alumina versus depth in the Delee No. 1 well, Hitchcock N.E. field.

Figure 19. Strontium versus chloride in formation water, Brazoria and Galveston Counties (data from Kharaka and others, 1977). Positions of the Prets No. 1 and Pleasant Bayou geopressured-geothermal test wells are shown for comparison. Normal evaporite curve from Collins (1975).

Figure 20. δD SMOW versus depth in formation water, Brazoria and Galveston Counties (data from Kharaka and others, 1977). Positions of the Prets No. 1 and Pleasant Bayou geopressured-geothermal test wells are shown for comparison.

Figure 21. Concentration of short chain aliphatic acids (C_2-C_5) versus depth in formation water, Brazoria and Galveston Counties (data from Kharaka and others, 1977). Positions of the Prets No. 1 and Pleasant Bayou geopressured-geothermal test wells are shown for comparison.

Figure 22. Key for pyrolysis data interpretation (Dow and Page, 1981) with average values from the Delee No. 1 well.

Figure 23. Van Krevelen diagram showing the source rock quality of Anahuac and Frio shales from the Delee No. 1 well.

Figure 24. Pyrolysis maturity diagram (T-Max°C versus S1/S1 + S2) showing immature nature of the Delee No. 1 shales.

Figure 25. Histograms of the canonical variable (CV) for $\delta^{13}C$ aromatics versus $\delta^{13}C$ saturates from Sofer (1984). The Prets No. 1 oil plots within the nonwaxy oils.

Figure 26. Canonical variable (CV) versus pristane/phytane (Pr/Ph) ratios. Taken from Sofer (1984). The position of the Prets No. 1 oil is shown.

Figure 27. Surface faulting and subsidence in the Caplen and Robinson Lake areas, as detected on 1982 aerial photographs taken for the General Land Office, and subsurface faults at about 7,000 ft from well data. Faults in East Bay from Verbeek and Clanton (1981, their fig. 3a).

Figure 28. Production of oil and gas versus depth in Caplen field through 1979. Data from International Oil Scouts Association (1983).

Figure 29. East Bay fault system compared with subsurface structure. The faults form grabens on subsurface highs rimming the Onion Bayou salt-withdrawal basin.

Figure 30. Stratigraphic section from Caplen to High Island, showing continuity of Lower Miocene sandstone reservoirs.

Figure 31. Genoa-Webster fault system compared with subsurface structure. These faults form grabens rimming the Genoa salt-withdrawal basin.